Addis Ababa University
Addis Ababa Institute of Technology
School of Electrical and Computer Engineering
Communication Engineering Graduate Program

PERFORMANCE ANALYSIS OF A MICROSTRIP ANTENNA FOR 5G APPLICATIONS USING METAMATERIAL

by:

Moti Indalew

Advisor:
Dr. Murad Ridwan

A Thesis Submitted to the School of Gradiauate Studies of Addis Ababa University in Partial Fulfillment of the Requirement for the Degree of Master's Science in Communication Engineering

October, 2024

Adis Ababa University
Addis Ababa Institute of Technology
School of Electrical and Computer Engineering
Communication Engineering Graduate Program

PERFORMANCE ANALYSIS OF A MICROSTRIP ANTENNA FOR 5G APPLICATIONS USING METAMATERIAL

by:

Moti Indalew

Approval by Board of Examiners	Signature	Date
Chairman, School Graduate Comittee:	_____	_____
Advisor's Name:	_____	_____
Internal Examiner's Name:	_____	_____
External Examiner's Name:	_____	_____

Declaration

I declare that this thesis is entirely my own work and does not include any content from other educational institutions without proper acknowledgement. To the best of my knowledge, it does not contain previously published material by another person without recognition.

Name of the Student	Signature	Date
_____	_____	_____

This thesis has been submitted for examination with my approval as a university advisor.

Name of the Advisor	Signature	Date
_____	_____	_____

Addia Ababa, Ethiopia

Abstract

Because of its low profile, low cost, and ease of fabrication in the circuit boards to construct smart cities using the internet of things (IOT), microstrip antennas have grown to be an important component of today's wireless communication world. The majority of 5th generation applications are incompatible with poor performance characteristics such narrow bandwidth, low power handling capability, low gain, and huge antenna footprint.

Different design optimization technique studies have been conducted to improve the bandwidth, gain, and size of microstrip antennas for recent generation networks, but the performance of these antennas is still need the enhancement of bandwidth for fifth generation applications and above. The primary goal of this research is to determine how metamaterials affect the bandwidth performance of microstrip antennas. CST Microwave Studio was used to design and simulate the antenna's structure, which works in the 28 GHz range. The Rogers RT Duroid 5880 material, which has a dielectric coefficient of 2.2, was used as the substrate for the antenna construction.

With an increase in turns, the metamaterial-based microstrip antenna's bandwidth expanded for every split ring resonator segmentation. Notably, it changed quickly from single turn to two turn, but only marginally after that. Compared to circular and triangular split ring resonator; rectangular split ring resonaror exhibit superior bandwidth augmentation. By etching the rectangular, circular and triangular split reing resonator, respectively, with N=3, the bandwidth is increased by 53.06%, 46.7% and 26.89% compared to the conventional microstrip antenna.

The bandwidth is enhanced by using more split ring resonators than by using just one.The bandwidth is increased by 101.81% when utilizing 2x2 split ring resonator elements compared to a conventional microstrip antenna without a split ring resonator.

The radiation efficiencies of conventional microstrip antennas, CSRR-based microstrip antennas, rectangular split ring resonator-based microstrip antennas, triangular split ring resonator-based microstrip antennas, and pentagonal split ring resonator-based microstrip antennas are 86 %, 87.9%, 85.3%, 80.3 % and 92.4 %, respectively.

Key Words:CST MWS; 5G; Mmwave ; High gain ; Microstrip antenna array; SRR.

Acknowledgments

First of all, I am thankful for the almighty of God for the good health and well-being that has enabled me to complete this work. I would like to express my sincere gratitude to my advisor Dr. Murad Ridwan for his continuous support, patience, motivation, understanding and immense knowledge. His guidance helped me in all the time of research and writing of this thesis. I am also very grateful to my family, colleagues, friends and others whom positively or negatively contributed in many ways for successful accomplishment of this thesis.

Table of Contents

List of Tables

List of Figures

List of Abbreviations

SRR	Split ring resonator
CST	Computer simulation technology
CSRR	Circular split ring resonator
D2D	device to device
ϵ_o	permitivity of free space
5G	fifth generations
IOT	internet of things
MIMO	multiple input multiple out put
Multi-RAT	muti radio access terrestrial
Mbps	mega bits per second
MTM	Metamaterial
PSRR	Pentagonal split ring resonator
μ	Permability of free space
RSRR	Rectangular split ring resonator
SRS	split ring resonator
Tbps	tera bits per second
TSRR	Triangular split ring resonator

Chapter 1: **Introduction**

1.1 Back Ground

The growing demand for telecommunications services is stimulating the development of wireless technologies. Each generation of mobile technologies has brought with it an increase in the data transmission speed along with improved connection quality and new functionalities. The fourth generation (4G) technology, which is currently in use, has been available worldwide since 2009. The fifth generation (5G) network will enable a number of new services, including those related to the Internet of Things (IoT) and the concept of smart cities.

In addition, 5G network emerges a new era for vehicular communication, device to device (D2D) communication and specially the IOT will be the most exciting technology that 5G will make happen. To address these features, telecommunication industry is introduce a number of enabling technologies such as mm wave system, multiple radio access technology (Multi-RAT), advanced multiple inputs multiple outputs (MIMO), advanced network, and advanced small cell etc. [2].

To make 5G able to support the features quoted before, there are many alternatives to go for higher frequency bands. For this purpose, a number of higher frequency bands are declared as 5G frequency bands such as 3.4–3.6 GHz, 5–6 GHz, 24.25–27.5 GHz, 27.5–28.35 GHz, 37–40.5 GHz and 66–76 GHz bands by International Telecommunication Union (ITU). Of these bands, 28 GHz band is carefully chosen for this research work and 28GHZ frequency band is already deployed in some places experimentally. [1].

Antennas are a fundamental component of any wireless communications systems. An antenna is a kind of transducer that converts a transmission line electrical signal into an electromagnetic wave in free space and vice versa. The technology related to antennas in the modern wireless system has been continuously improved with the corresponding increase in the number of requirements for communications. Compared to other antenna options, printed antennas have some excellent features, such as low profile, low weight, and are easy to manufacture, along with good performance characteristics. [1]. The unique properties of printed antennas, such as mechanical conformability, durability, compactness, and cheap manufacturing costs make them suitable for many applications. Printed antennas have a range of applications in the commercial, medical, military, and aerospace sectors, and are often mounted on the exterior of spacecraft and aircraft as well as incorporated into wireless devices. In addition, the straightforward integration of printed antennas with electronics systems has opened new fields of application, such as 5G phased array and smart sensing systems [2].

The rectangular patch antenna is very probably the most popular microstrip antenna design implemented by designers. Figure1 shows the geometry of this antenna type. A rectangular metal patch of width W = a and length L = b is separated by a dielectric material from a ground plane by a distance h. The two ends of the antenna (located at 0 and b) can be viewed as radiating due to fringing fields along each edge of width W (= a). The two radiating edges are separated by a distance L (= b). The two edges along the sides of length L are often referred to as non radiating edges. [3]

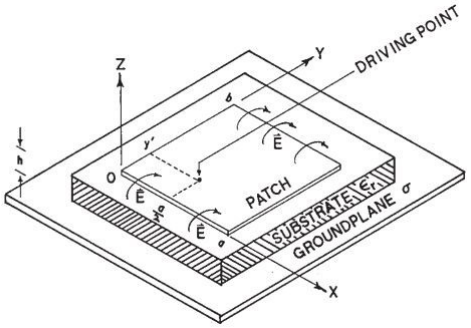

Figure 1.1: Rectangular microstrip patch geometry used to describe the transmission line model

Metamaterials are artificially designed structures or materials with qualities that vary from those found in nature. The electromagnetic (EM) properties of these materials or mediums are described by electric permittivity (ϵ) or magnetic permeability (μ.) Permittivity and permeability are terms that describe how a material behaves in electric and magnetic fields, respectively. These characteristics might be either positive or negative. When both permittivity and permeability are negative, the material is referred to as a double negative (DNG), which is synthetic and not found in nature.

Materials having positive epsilon and mu are referred to as double positive (DPG). These properties may be seen in many plasmas. Furthermore, if the material's permittivity is positive, it is referred to as epsilon positive (EPG) material. Negative permeability materials, on the other hand, are referred to as μ negative materials (MNGs). Single negative material (SNG) is another name for epsilon or mu negative material.

1.2 Problem of Statement

Patch antennas have a lot of benefits, but they also have some serious disadvantages. The design of compatible microstrip antennas for many purposes has advanced significantly, but it is still bandwidth of microstrip antenna is limited. This research primarily focuses on analyzing how metamaterial influences the performance compact microstrip antennas for a variety of applications.

1.3 Objective

1.3.1 General objective of the study

The major goal of this thesis is to identify impact of metamaterial on performance enhancements in microstrip antennas suitable for 5G applications.

1.3.2 Specific objectives of the study

(a) Design conventional microstrip patch antenna at 28GHz.

(b) Performance analysis and simulation is done with CST mws software.

(c) Design and performance analysis of metamaterial based microstrip patch antenna at 28 GHz for different segmentation of split ring resonator.

(d) Performance comparison and Result discussion of metamaterial-based antenna with existing conventional microstrip antenna.

1.4 Scope of the research

The advantage of metamaterial in the design and analysis of microstrip antenna tiny for 5G use is discussed in this thesis work in order to create low-profile, high-performance microstrip patch antenna. MWS, a computer simulation technology, simulates the outcome. Based on the simulation results, a comparison with the current micro strip antenna is done.

1.5 Methodology

Literature review: The first phase is research phase at the beginning is gathering basic knowledge on the topic and arrangement of collecting data. Includes reading books, journals, and related work. Design and mathematical analysis: Based on an idea, the proposed antenna would be designed, numerical analysis for different radiation parameters such as return loss, gain, pattern and VSWR.

Simulation and interpretation of the result: we can simulate the proposed antenna in CST MWS to get the performance the microstrip antenna radiation parameters such as bandwidth, gain, pattern and parameters. Performance comparison: It will be held between currently designed metamaterial based microstrip antennas and already deployed conventional microstrip antenna and proposed in different literature.

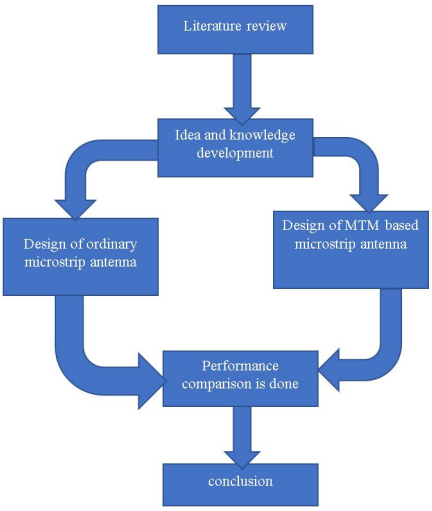

Figure 1.2: flow chart of methodology

1.6 Literature Review

There are many researches works related to designing high performance microstrip antenna operating at 28 GHz band as this band is the experimental launched for 5G wireless network. It's a challenge for the antenna engineers which have led them to suggest several antennas outlined below.

Comparative Study of square and circular split ring resonator metamaterial for patch antenna miniaturization for C-band wireless applications research contribute square split ring resonator metamaterial provides slightly more miniaturization compared to circular split ring resonator but the research only considers for single turn of split ring resonator. It does not study the impact of number of turn. [4]

The proposed antenna in [5] an array antenna is designed whose size is small enough to use inside the mobile phones and also it have good gain to support for 5G application. In [6] This article presents the design of a planar MIMO (Multiple Inputs Multiple Outputs) antenna comprised of two sets orthogonally placed 1 $\times$ 12 linear antenna arrays for 5G millimeter wave (mmWave) applications. Wideband Aperture Coupled Stacked Microstrip Antenna at 28 GHz for 5G Applications is designed in [7] . This research enhances very good bandwidth and gain. The arrays are made of probe-fed microstrip patch antenna elements on a 90 $\times$ 160 mm2 Rogers RT/Duroid 5880 grounded dielectric substrate achieve a gain of 12 dBi which is quite large to be implemented inside the mobile phone. In [8] The dimensions of the overall substrate used in MIMO configuration are L = 130 mm $\times$ W = 65 mm. which is enhanced the gain up to 12.8 dB by adopting a four elements array configuration this array have good gain performance but still antenna dimension required to minimize to fit for small size electronics communication. A Microstrip Antenna Using I-Shaped Metamaterial Superstrate with Enhanced Gain for Multiband Wireless Systems is designed in [9] have a bandwidth of 240Mhz to 1.1Ghz but The bandwidth enhancement is performed with the cost increasing antenna array dimension that is incompatible with handheld electronics device.

The antenna reported in [11] is an 8-element array, accomplished a peak gain of 12 dBi while its size is 66 × 15 mm2 which is large and the design is very complex. An array antenna comprising of 8 elements is designed by the researchers in the literature [12], is reconfigurable antenna array used for different mode operation such as diversity or cognitive radio communication which attained maximum gain of 9.57 dBi at 28 GHz while it needs 8 different ports for 8 antenna array elements which make it very expensive design and have large antenna size The overall size of the antenna is 60 x120 mm2. A 1×4 microstrip patch antenna array operated at 28 GHz covering 5G frequency band is designed in [13]. The maximum gain achieved by the antenna array is 13.04 dBi at 27.8 GHz with very good operational band width but antenna size still to large (20x57.4 mm.2).

1.7 Thesis Organization

This thesis is composed of five chapters and the overview of each chapter is as follows: Chapter 1: The introduction, problem statement, objective, methodology and literature reviews on the patch antennas and metamaterial concept are discussed on this chapter.

Chapter 2: This chapter presents the fundamental antenna parameters, review on the theory of metamaterial science and microstrip patch antenna.

Chapter 3: This chapter discusses the analysis and design of the patch antennas which operates at mm-wave frequency specifically at 28 GHz and design of split ring resonator.

Chapter 4: The simulation results obtained on both conventional microstrip patch antenna and metamaterial based microstrip antenna for different segmentation of split ring resonator one by one are discussed and compared in this chapter.

Chapter 5: Conclusion of the thesis and suggestions for future work are presented in this final chapter.

Chapter 2: Antenna Parameters and Metamaterail Based Antenna Technology

2.1 Overview of Antenna Parameters

To describe the performance of an antenna, definitions of various parameters are necessary. Some of the parameters are interrelated and not all of them need be specified for complete description of the antenna performance. Parameter definitions will be given in this chapter. [14]

2.1.1 Radiation Pattern

An antenna radiation pattern or antenna pattern is defined as "a mathematical function or a graphical representation of the radiation properties of the antenna as a function of space coordinates. In most cases, the radiation pattern is determined in the far field region and is represented as a function of the directional coordinates. Radiation properties include power flux density, radiation intensity, field strength, directivity, phase or polarization.

The radiation property of most concern is the two- or three-dimensional spatial distribution of radiated energy as a function of the observer's position along a path or surface of constant radius. A convenient set of coordinates is shown in Figure 2.1. A trace of the received electric (magnetic) field at a constant radius is called the amplitude field pattern. On the other hand, a graph of the spatial variation of the power density along a constant radius is called an amplitude power pattern. [13] Often the field and power patterns are normalized with respect to their maximum value, yielding normalized field and power patterns. Also, the power pattern is usually plotted on a logarithmic scale or more commonly in decibels (dB). This scale is usually desirable because a logarithmic scale can accentuate in more details those parts of the pattern that have very low values, which later we will refer to as minor lobes. [14] For an antenna, the

(a) field pattern (in linear scale) typically represents a plot of the magnitude of the electric or magnetic field as a function of the angular space.

(b) power pattern (in linear scale) typically represents a plot of the square of the magnitude of the electric or magnetic field as a function of the angular space.

(c) power pattern (in dB) represents the magnitude of the electric or magnetic field, in decibels, as a function of the angular space

2.1.2 Return Loss

It is a parameter that is used to measure the power reflected by the antenna due to the mismatch of the transmission line and antenna. Thus, the return loss is a parameter

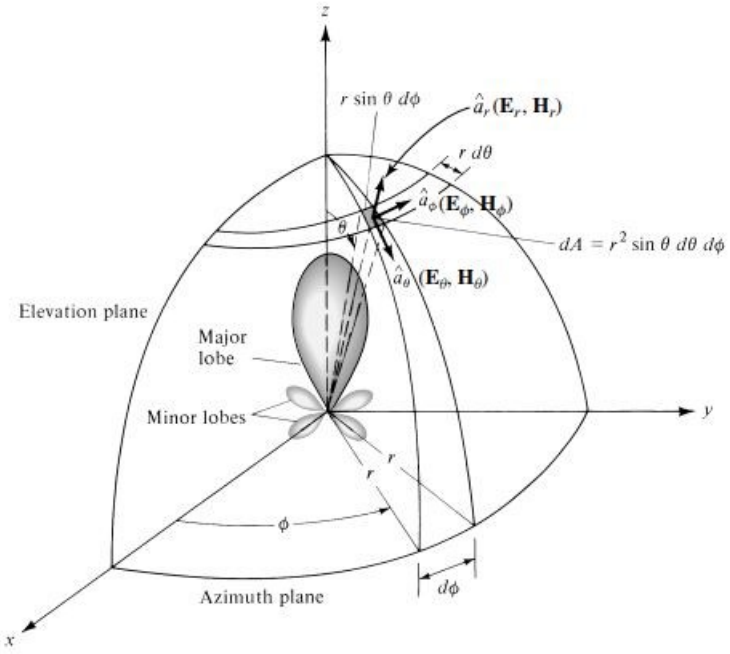

Figure 2.1: Coordinate system for antenna analysis. [14]

like the VSWR to demonstrate how well the matching between the transmitter and receiver has occurred. Its measurement describes the ratio of the reflected power in the reflected wave to the power in the incident wave in units of decibels. [15] where return loss is given by

$$ReturnLoss = 20log|\gamma|(dB) \tag{2.1}$$

Where $|\gamma|$ represents the magnitude of the reflection coefficient and this value is always below 1. For ideal matching between the transmitter and the receiver, $= 0$ and $R_L = \infty$ which implies no power would be reflected back, whereas a $\gamma = 1$ has a RL = 0 dB, which implies that there is nothing to radiate by the antenna because the power provided to the antenna is completely reflected.

The Return Loss can also be calculated from the VSWR using the equation 2.9. Note that return loss is given as a ratio expressed in decibels.

$$Returnloss = -20 \log \frac{VSWR - 1}{VSWR + 1} db \tag{2.2}$$

The return loss is given as a negative figure. Being a loss, the returned power must be less than the forward power, and hence the return loss has a minus sign or negative figures of decibels represent a loss.

2.1.3 S-parameters

The S-parameters are very important in microwave design for describing the behavior of electrical devices. Most of the electrical properties i.e. VSWR, return loss, gain and so on relates to the S parameters. S-parameters characterizes the input and output relationship between ports in an electrical system. The S-parameters S11 and S22 represent input and output reflection while S21 is the forward transmission coefficient (gain) and S12 are the reverse transmission coefficient (isolation) which measures the power transferred from port 1 to port 2. [16] S11 (sometimes written as return loss) represents how much power is reflected from the antenna, and hence is known as the reflection coefficient. If S11 = 0 dB, then all the power is reflected from the antenna and nothing is radiated.

2.1.4 Bandwidth

The bandwidth of an antenna is defined as "the range of frequencies within which the performance of the antenna, with respect to some characteristic, conforms to a specified standard." The bandwidth can be considered to be the range of frequencies, on either side of a center frequency (usually the resonance frequency for a dipole), where the antenna characteristics (such as input impedance, pattern, beam width, polarization, side lobe level, gain, beam direction, radiation efficiency) are within an acceptable value of those at the center frequency. For broadband antennas, the bandwidth is usually expressed as the ratio of the upper-to-lower frequencies of acceptable operation. For example, a 10:1 bandwidth indicates that the upper frequency is 10 times greater than the lower. For narrowband antennas, the bandwidth is expressed as a percentage of the frequency difference (upper minus lower) over the center frequency of the bandwidth.

For example, a 5% bandwidth indicates that the frequency difference of acceptable operation is 5% of the center frequency of the bandwidth. [14]

$$BW = 100 * \frac{F_H - F_L}{F_C} \tag{2.3}$$

Where, FH is the highest frequency,

FL is the lowest frequency, and

FC is the center frequency in the band.

2.2 Metamaterail Based Antenna Technology

2.2.1 Back ground of Metamaterial

The term of metamaterial was synthesized by Rodger M. Walser, University of Texas at Austin, in 1999, which was originally defined as "Macroscopic composites having a synthetic, three-dimensional, periodic cellular architecture designed to produce an optimized combination, not available in nature, of two or more responses to specific excitation". [17] Based on Wikipedia, the metamaterial is defined as "a material which gains its properties from its structure rather than directly from its composition" [17].

The above definitions reflect certain natures of metamaterial, but not all. Actually, a metamaterial is a macroscopic composite of periodic or non-periodic structure, whose function is due to both the cellular architecture and the chemical composition. If the metamaterial is regarded as an effective medium, there is an additional requirement that the cellular size is smaller than or equal to the subwavelength. The metamaterials are required to have sub-wavelength for the unit cell so that they can be described using the effective medium theory. Figure 2.2 shows two typical metamaterial structures in the microwave regime, in which Fig. 2.2(a) is a periodic structure that is equivalent to a homogeneous medium and Fig. 2.2 (b) is a non-periodic structure that is equivalent to an in homogeneous (gradient) medium.

The microwave metamaterials are fabricated with printed circuit boards (PCB) by making different metal architectures on PCB. The properties of such metamaterials are mainly due to the cellular architecture, and also dependent on the PCB substrates, which can be FR4 and Rogress RT. The dependence of metamaterial properties on the cellular architecture provides great flexibility to control metamaterials. One can create new materials which are unavailable in nature but can be realized in practice using metamaterial structures. This is the biggest advantage of metamaterials.

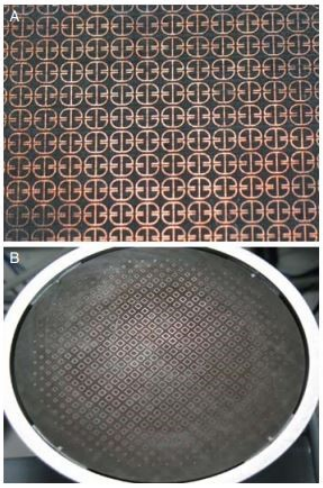

Figure 2.2: Two typical metamaterial structures in the microwave regime. (a) A periodic structure, which is equivalent to a homogeneous medium (above). (b) A non-periodic structure, which is equivalent to an inhomogeneous (gradient) medium (below).

Usually, the material properties are characterized by an electric permittivity (ϵ) and a magnetic permeability (μ). The thinnest material in nature is free space or air, whose permittivity is (ϵ_o) and permeability is (μ_0). The relative permittivity and permeability of a material are defined as $\epsilon_r = \frac{\epsilon}{\epsilon_o}$ and $\mu_r = \frac{\mu}{\mu_o}$, respectively, which define another important material parameter, the refractive index, as$n = \epsilon_r \mu_r$.

In nature, most materials have the permeability μ_0 and permittivity larger than ϵ_0. The metamaterial opens a door to realize all possible material properties by designing different cellular architectures and using different substrate materials.

Figure 2.3 illustrates all possible properties of isotropic and lossless materials in the ϵ– domain. In Fig. 2.3, the first quadrant ($\epsilon > 0 and \mu > 0$) represents right-handed materials (RHM), which support the forward propagating waves. From the Maxwell's equations, the electric field E, the magnetic field H, and the wave vector k form a right-handed system. The second quadrant ($\epsilon < 0 and \mu > 0$) denotes electric plasma, which support evanescent waves. The third quadrant ($\epsilon < 0 and \mu < 0$) is the well-known left-handed materials (LHM), which was proposed by Veselago in 1968 supporting the backward propagating waves. In LHM, the electric field E, the magnetic field H, and the wave vector k form a left-handed system. The fourth quadrant ($\epsilon > 0 and \mu < 0$) represents magnetic plasma, which supports evanescent waves.

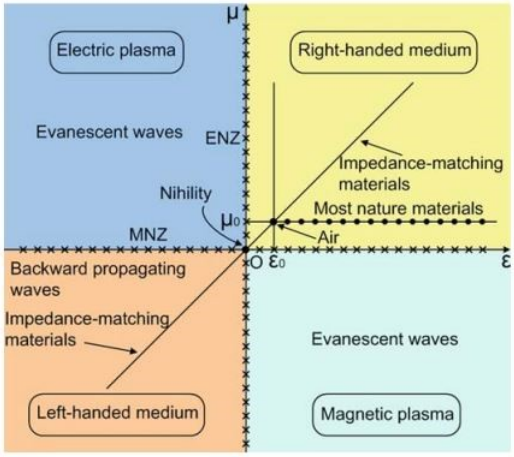

Figure 2.3: All possible properties of isotropic materials in the –u domain.

In Fig. 2.3, most natural materials only occur at certain discrete points on the line $\mu = \mu_0$ and $\epsilon\epsilon_o$, and seldom natural electric plasma and magnetic plasma occur in very small parts in the second and fourth quadrants. Most of material properties have to be realized using metamaterials, even for RHM. In a long period, metamaterials, LHM, negative-refractive index materials (NIM), double negative materials (DNG), and backward-wave materials have been regarded as the same terms. However, they actually represent different meanings. Metamaterials have much broader scope than LHM, as shown in Fig. 2.3.

In the ϵ–$\mu domain$, there are several special lines and points indicating special material properties. For example, the point $=_0$ and $\epsilon = \epsilon_o$represents an anti-air in the LHM region which will produce a perfect lens; the point $u = 0and\epsilon = 0$ represents a nihility , which can yield a perfect tunneling effect; the line $\mu = \epsilon$ in both RHM and LHM regions represents impedance-matching materials, which have perfect impedance matching with air resulting no reflections. Also, the vicinity of $\mu = 0$ is called as -near zero (MNZ) material, and the vicinity of $\epsilon = 0$ is called as -near zero (ENZ) material which has special properties.

Actually, metamaterials have much more features beyond those shown in Fig. 2.3. Metamaterials can be designed as weakly and highly anisotropic, depending on different requirements. The flexibility to design various material properties together with the optical transformation makes it possible to control electromagnetic waves at will using metamaterials. [18]

2.2.2 Classification of materials

One way of classification of natural and MTM is based on the propagation phase constant (β) of the current flowing through the antenna element [19]. The material is classified as natural if the value of β is greater than zero ($\beta > 0$). For example, Figure 2.4a illustrates the antenna where the flow of current from feed point F has phase constant positive ($\beta > 0$). The phase distribution in such antenna receipts a regressive form, resulting in a lag of phase from point F to antenna ends. The material is classified as MTM if the value of $\beta is less than zero (\beta < 0)$ for a particular frequency band or zero at the nonzero frequency $(\beta = 0). For example, Figure 2.4b illustrates the \beta of the outgoing current is negative (\beta < 0)$ within a particular band of frequency or zero at the frequency of non-zero ($\beta = 0$). The phase distribution in such antenna receipts a progressive form from point F to antenna ends and $\beta = 0$] indicates infinite long wavelength. This kind of antenna is classified into an MTM antenna or MTM-based antenna

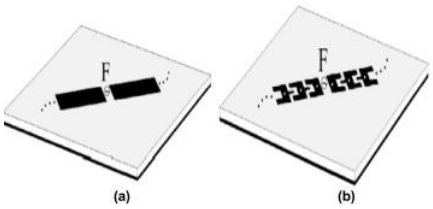

Figure 2.4: flow of current from feed point f.

MTM

The electric permittivity (ϵ) and magnetic permeability (μ) are used to characterize an electromagnetic material. [20] The right-handed (RH) material having $\epsilon > 0$ and $\epsilon > 0$ demonstrates the phase constant of wave propagation (β) to be a positive value ($\beta > 0$) and is termed as double-positive (DPS) material. The single negative material such as epsilon negative (ENG) having $< 0 and \mu > 0$, and μ negative (MNG) having $\epsilon > 0$ and $\mu < 0$) exhibits phase constant of wave propagation is zero ($\beta = 0$evanescent). The left-handed (LH) material having $\epsilon < 0 and \mu < 0$ demonstrates the phase constant of wave propagation to be a negative value ($\beta < 0$) and is termed as double negative (DNG) material. An RH material is easily found in nature, whereas ENG, MNG, DNG materials are artificial and referred to as MTM.

2.2.3 Metamaterials in antenna design

One of the most important applications of metamaterials is antenna design. Due to the unusual properties of metamaterials, we can achieve antennas with novel characteristics which cannot be realized with traditional materials. In this section, several types of metamaterial loaded antennas will be reviewed.

Electrically small antennas based on zeroth resonant mode

In mobile communication systems, electrically small antennas (ESA) are desired. Modern integrated circuit technology has the ability to miniature circuits to a very small size. However, in a traditional design, the performance of the antenna is related with its

size. The antenna usually has dimensions in the order of the operating wavelength. This sets boundaries for the size of the whole system. [22] A ZIM medium, whose refractive index is near zero, shows an operating wavelength that is infinite at an arbitrary designed frequency. This phenomenon is named zeroth resonant mode.Since the wave number in this antenna is zero, in theory, the physical size of the antenna can be made independent of its working frequency. Because the operating wavelength is infinite, the field distribution and the radiation pattern are different from the normal ones. [23]

Dual-band and multi-band antennas

Normal dual-band antennas are realized with different resonant structures, or different resonant modes in one structure. The main disadvantage of this technique is that the field distributions in these structures can hardly be the same in both bands.

This means that the radiation patterns in the operating bands are different. [24] Since metamaterials can support a negative refractive index, the resonant modes can be selected as a symmetric pair, i.e. so-called negative and positive modes. The field distributions of these two modes can be very similar, and thus also the radiation patterns. [25] Negative and positive modes can be designed together with a zeroth-order mode. This yields a multi-band antenna with a specific pattern for each mode. An extra advantage of a metamaterial-loaded multi-band antenna is the fact that its size is usually smaller than in a traditional design, where the size is decided by the lowest operating frequency. [24]

Low Profile planar reflectors

In an electric dipole antenna positioned parallel on top of a PEC plane, the distance between the dipole antenna and the reflector should be approximately a quarter wavelength. Indeed, since the reflective phase at the PEC plane is 180°, the radiation of the image of the electric dipole will start to cancel the radiation of the dipole itself if it is located closer to the reflector. However, if the reflector is a PMC plane, the reflective phase is zero, and the image of the electric dipole will enhance the radiation when the dipole is located near the PMC plane. This technique allows designing low profile reflectors for electric dipole antennas. Conversely, magnetic dipoles, in practice realized by slots or apertures in a ground plate, are also not suitable for placement near any PEC plane because of the generation of parallel plate modes between the two metal planes, which considerably distorts the characteristics. An AMC plane can help to suppress any parallel plate modes. Also in this case, low profile structures become feasible. [26]

Antenna lenses and polarizers

Dielectric lenses can be used to improve the directivity and gain of an antenna. However, the cost to fabricate a 3D lens is large. Further, the location of the lens should be carefully chosen in relation with the phase center of the antenna. A metamaterial lens can be formed by a flat 2D structure. Their manufacturing cost is much lower. They can even be integrated with the planar antenna structure to reduce the profile and size of the antenna system. [27]

A polarizer can be based on a chiral medium which has the capability to transform

a linearly polarized wave into a circularly polarized wave. This opens a way to design circularly polarized antennas based on existing linearly polarized antennas. [26]

2.2.4 Spiral resonators as artificial magnetic materials

Artificial magnetic materials (AMMs) are composed of metallic inclusions showing a high magnetic polarisability (μ-dispersive behavior), hence, they are usually referred to as magnetic resonators. Split-ring resonators (SRRs) were first introduced by Pendry [18] as they provide the required MNG behavior to realize DNG metamaterials. However, other well-known magnetic resonators are the spiral resonators (SRs). Additional geometries can also be found in the literature such as the capacitively loaded loops (CLLs) and the omega particles (Ω) [27].

It is also interesting that some magnetic resonators like the SRRs introduce undesired cross polarization or bianisotropic effects, that is, an electric polarization may be created when a magnetic field is applied, and vice versa. Bianisotropy is characterized by different forward and backward reflected powers (or different reflection S-parameters), wider stop-band in transmission, and the presence of a magneto-electric coupling coefficient (0). The bianisotropy present in the SRRs comes from the different dimensions of the internal and external rings; this results in an additional electric polarizability. A modified SRR was proposed in to avoid the bianisotropy present in the typical SRRs. This was the so-called broadside-coupled SRR (BC-SRR), and it consists of two identical rings placed on both sides of the dielectric substrate that cancel the magneto-electric coefficient, and hence, there is no bianisotropy in this magnetic resonator.[28].

Chapter 3: Design and Analysis of Conventional and Metamaterial Based Microstrip Antenna

3.1 Designing of conventional microstrip Patch antenna

To design a rectangular microstrip patch antenna the essential parameters are operating frequency of the antenna (f_r), the relative dielectric constant of substrate ($_r$) and thickness of the dielectric substrate (h). The choosing of these design parameters is important because the dimensions of a rectangular microstrip patch antenna and antenna performance depends on these parameters.

To have a big data rate for 5G mobile communication, the resonant frequency selected for the design is 28 GHz. The dielectric material selected for the design is RT5880 (lossy) which has a dielectric constant of 2.2. For the microstrip patch antenna to be utilized in mobile phones, it is essential that the antenna is not massive. Hence, the height of the dielectric substrate is selected as 0.28 mm.

The Performance of the microstrip antenna depends on its dimension. The radiation efficiency, return loss, gain, directivity and other related parameters are affected depending on the dimension of the patch. For an efficient radiation, the practical width of the patch can be calculated as.

The Patch Width (W):

The practical width of the patch used is calculated using below equation.

$$W = \frac{C}{2f\sqrt{\frac{\epsilon_r+1}{2}}} \tag{3.1}$$

Where, c is speed of light, which is equal to 3 × 108m/s,

ϵ_r is the relative dielectric constant of substrate

fo is the operating frequency in Hz, W is the width of the patch element Once we have c = 3 × 108 m/s, $\epsilon_r = 2.2$ and $f_o = 28$ GHz, The corresponding value of the width becomes:

$$W = \frac{3 * 10^8}{(2 * 28 * 10^9\sqrt{\frac{2.2+1}{2}}} = 4.232mm \tag{3.2}$$

The Effective Dielectric Constant (ϵ_{reff}):

Equation 3.3 is used to determine the effective dielectric constant of the microstrip patch antenna.

$$\epsilon_{reff} = \frac{\epsilon_r + 1}{2} + \frac{\epsilon_r - 1}{2}[1 + 12\frac{h}{w}]^{-\frac{1}{2}} \tag{3.3}$$

$$\epsilon_{reff} = \frac{2.2+1}{2} + \frac{2.2-1}{2}[1 + 12\frac{0.28}{4.232}]^{-\frac{1}{2}} = 2.1 \tag{3.4}$$

Here,$\epsilon_{reff}$is the effective dielectric constant and h is the height of dielectric substrate

The Effective Length (L_{eff}):

The length of the patch looks electrically slightly larger than the usual length of design, because of the fringing field along the patch width, and this parameter can be calculated by using equation 3.5:

$$L_{eff} = \frac{C}{2f_o\sqrt{\epsilon_{reff}}} \tag{3.5}$$

Substituting the values c = 3 × 108 m, f = 28 × 109 GHz and E_{reff} = 2:1, We get:

$$L_{eff} = \frac{3 * 10^8}{2 * 28 * 10^9\sqrt{2.1}} = 3.69mm \tag{3.6}$$

Calculation of the length extension (ΔL) :

Due to the fringing fields along the antenna it is appropriate to use extended length for a better performance. The length is extended by (ΔL) given by the equation 3.7

$$\Delta L = 0.412 * h\frac{\epsilon_{reff} + 3\frac{w}{h} + 0.264}{\epsilon_{eff} - 0.258\frac{w}{h} + 0.8} \tag{3.7}$$

Obtaining E_{eff} = 2.1 mm, W = 4.235 mm and h = 0.28 mm, then the length extension becomes:

$$\Delta L = 0.412 * 0.28 \frac{2.1 + 3\frac{4.232}{0.28} + 0.264}{2.1 - 0.258\frac{4.232}{0.28} + 0.8} = 0.077mm \tag{3.8}$$

Calculation of actual length of patch (L):

After the calculation of each of effective and extended lengths of the patch, the actual value of the radiating patch length (L) is calculated by using below equation.

$$L = L_{eff} - 2\Delta L \tag{3.9}$$

$$L = 3.69mm - 2 * 0.077mm = 3.448mm \tag{3.10}$$

The patch thickness, t is chosen to be very thin such that t 0 and for this case it is selected at t = 0.077 mm which is one of the standard thickness dimensions at mm wave frequency.

Calculation of the ground plane dimensions (L_g and W_g):

The transmission line model is applicable to infinite ground planes only. However, for practical considerations, it is basic to have a finite ground plane. It is shown by [3.11] that comparable outcomes for finite and infinite ground plane can be acquired if the size of the ground plane is greater than the patch dimensions by approximately six times the substrate thickness all around the periphery. Hence, for this structure, the ground plane measurements would be given as:

$$L_g = 6h + L \tag{3.11}$$

$$L_g = 6 * 0.28 + 3.448 = 4.93mm \tag{3.12}$$

$$w_g = 6h + w \tag{3.13}$$

$$w_g = 6 * 0.28 + 4.232 = 5.8mm \tag{3.14}$$

Where, L_g and W_g are the length and width of the ground plane, h is the height of the substrate, L and W are the length and width of the patch element respectively.

Equations below are used to determine the dimension of the ground plane, there's no need for the calculation of the dimension of the substrate because their dimensions are similar with that of the ground plane.

i.e. $L_s = L_g$ = 6h + L and $W_s = W_g$ = 6h + W.

Where, L_s and W_s are the length and width of the substrate.

After determining the dimensions of the rectangular patch, one should consider the feeder type. Here, microstrip line method is chosen as a feeding technique since it is easy to fabricate and control the feeding position.

Design parameter of microstrip patch antenna

Table 3.1: Design parameter of microstrip patch antenna

Symbol	Description	Value (mm)
W_p	Width of the patch	4.235
L_p	legth of the patch	3.536
W_s	Width of the substrate	5.135
L_s	Length of the substrate	4.432
l_f	length of the feed line	0.45
W_f	width of the feed line	0.37
h	Substrate thickness	0.28
t	Thickness of patch	0.077

3.2 Designing of MTM based Microstrip Patch Antenna

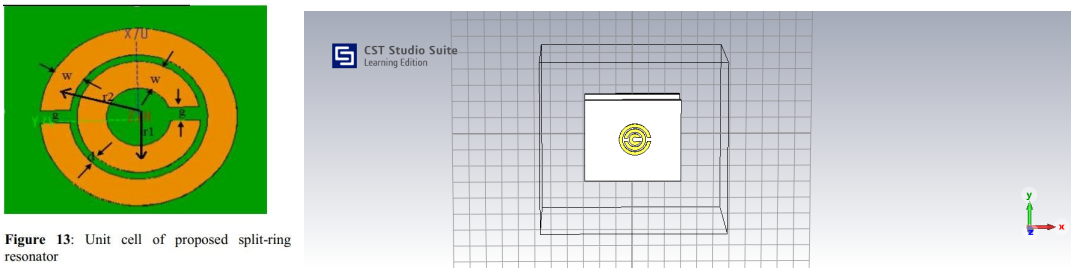

Figure 13: Unit cell of proposed split-ring resonator

Figure 3.1: Unit cell of proposed split ring resonator

Table 3.2: Design parameter for split resonator ring

Symbol	Description	Value (mm)
R_1	Radius of inner concentric ring	4.235
$R_1 1$	Radius of outer concentric ring	3.536
d	The gap between two concentric ring	5.135
w	Width of concentric ring	4.432
g	The gap for each concentric ring	0.45
h	Substrate thickness	0.28
t	Thickness of patch	0.077

Chapter 4: **Simulation Result and Discussion**

4.1 For conventional microstrip patch antenna

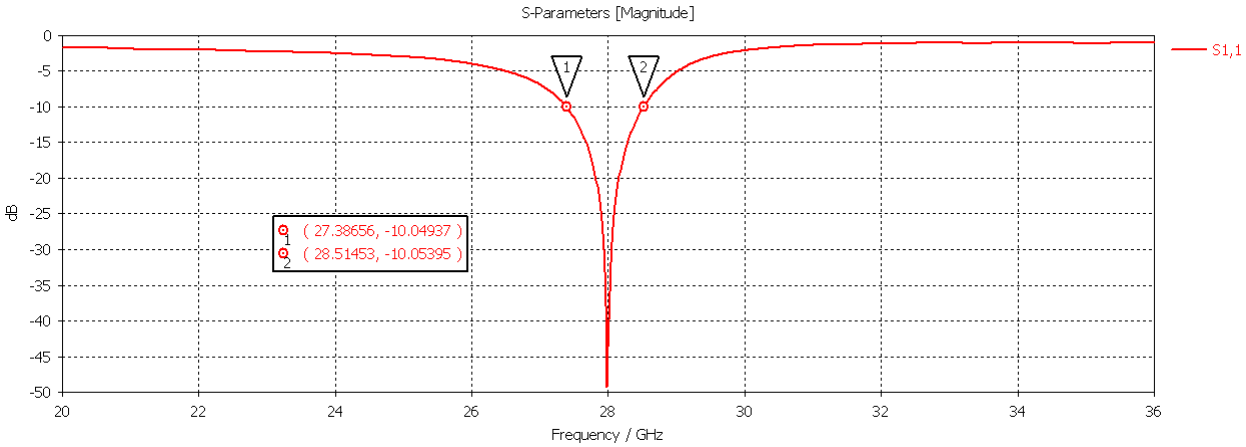

Figure 4.1: S-parameter of conventional microstrip antenna

As a result of the simulation, the conventional microstrip antenna's S-parameter, shown in Figure 4.1, indicates that the return loss at the frequency center, 28 GHz, is -43 db. The antenna's operating frequency ranges from 27.39 GHz to 28.5145 GHz, with corresponding to a bandwidth of 1.127 GHz (4.02%).

Radiation efficiency of conventional microstrip antenna 86% and total efficiency of the conventional microstrip antenna 85.99%.

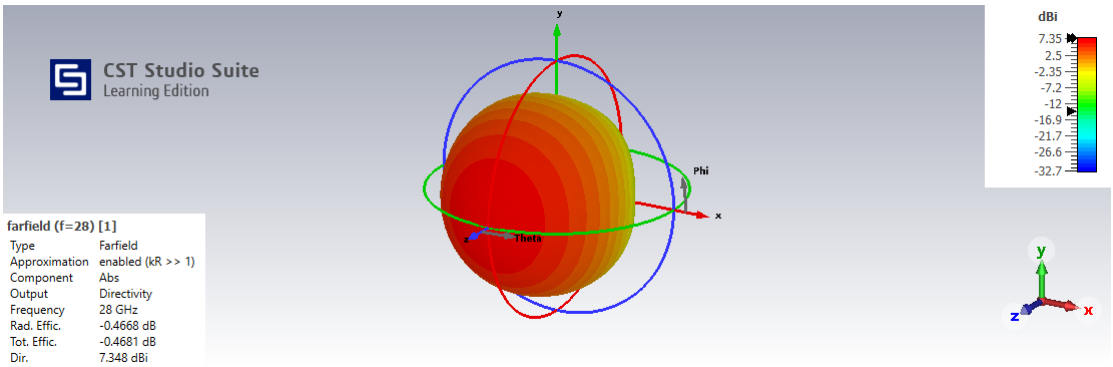

Figure 4.2: directivity of conventional microstrip antenna

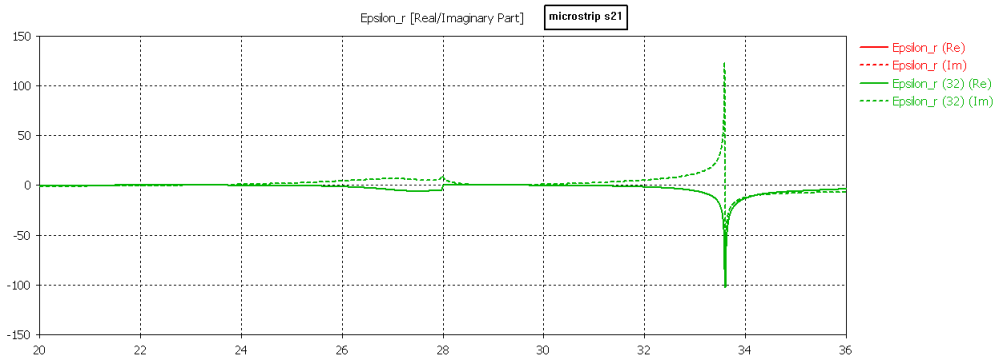

Figure 4.3: permitivty of conventional microstrip antenna

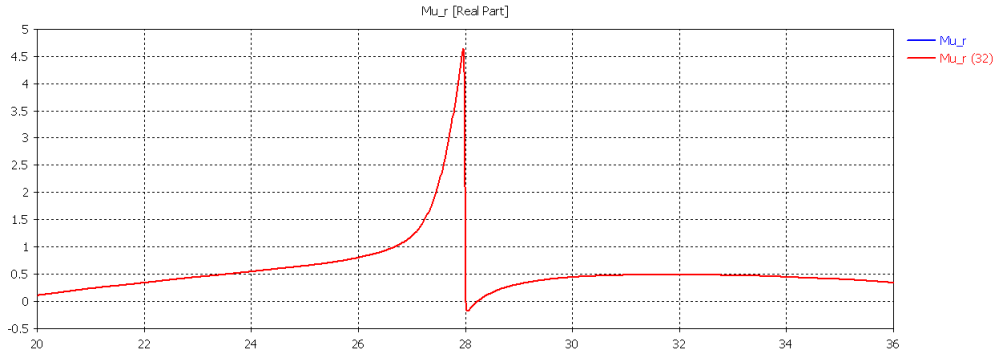

Figure 4.4: permability of conventional microstrip antenna

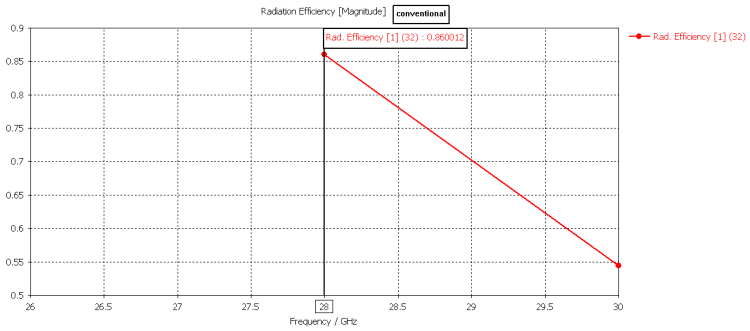

Figure 4.5: radation efficiency of conventional microstrip antenna

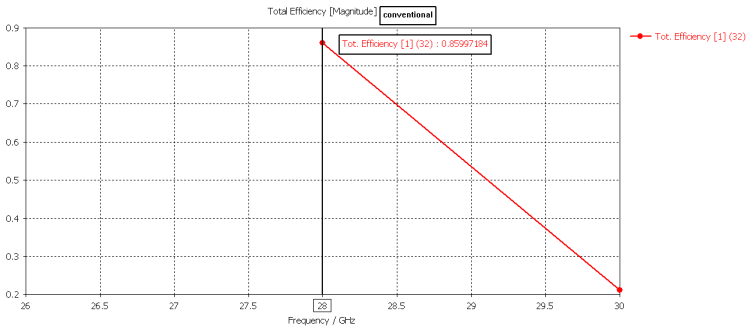

Figure 4.6: total efficiency of conventional microstrip antenna

4.2 Metamaterial-based microstrip antenna performance comparison with different segmentations split ring resonator

4.2.1 Circular split ring resonator based microstrip patch antenna

for N=1

Circular split ring resonator-based microstrip antennas with single turns operate at 28 GHZ have a bandwidth of 1.36 GHz (4.857%), with a frequency range of 27.205 GHz to 28.565 GHz. In comparison to a traditional microstrip antenna, the bandwidth was increased by 20.67 % have additional 0.233 GHz bandwidth.

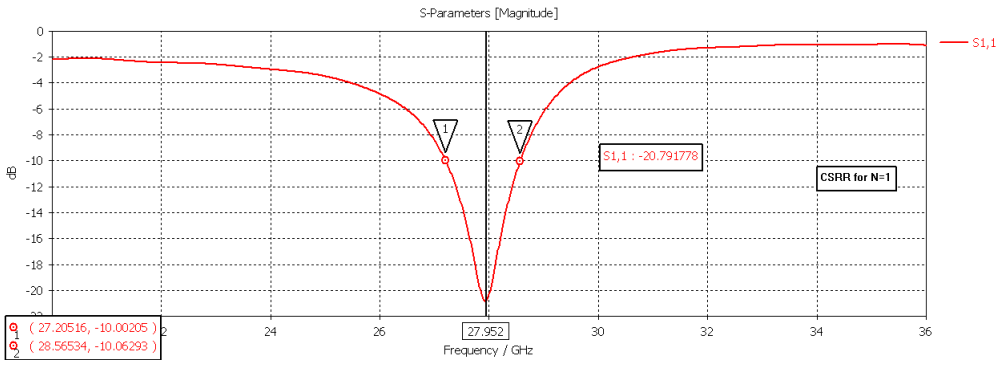

Figure 4.7: S-parameter of circular split ring resonator based microstrip antenna for N:1

for N:2

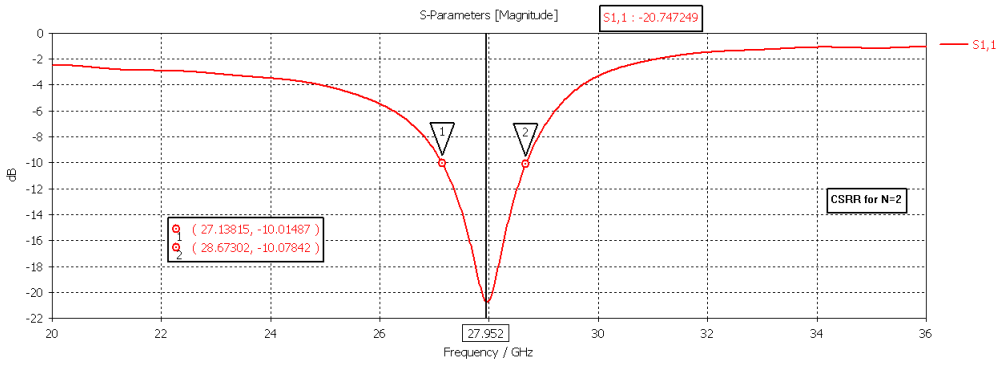

Figure 4.8: S-parameter of circular split ring resonator based microstrip antenna for N=2

Two-turn circular split ring resonator-based microstrip antennas span a frequency range of 27.138 GHz to 28.673 GHz, have operating bandwidth of 1.535 GHz (4.857%), the bandwidth was enhanced by (0.48GHZ) 36.2% as compared to a conventional microstrip antenna. When compared to a split ring resonator with a single turn, the bandwidth increased by 12.86% for microstrip antennas with two turns of CSRR.

for N=3

Three-turn circular split ring resonator microstrip antennas operate on in the frequency range of 27.089 GHz to 28.74 GHz and have an operating bandwidth of 1.652 GHz (5.9%). Compared to a conventional microstrip antenna, the bandwidth was increased by (0.525GHZ) 46.7%. Microstrip antennas with two turns of CSRR had a 7.62% increase

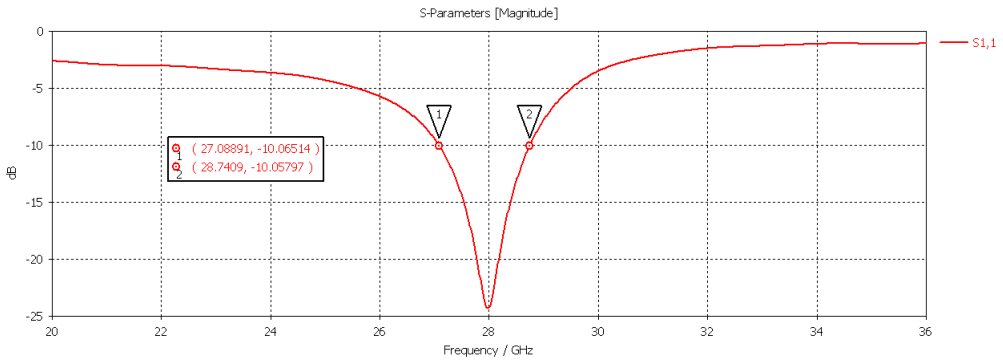

Figure 4.9: S-parameter of circular split ring resonator based microstrip antenna for N=3

in bandwidth when compared to a split ring resonator with two turns. The bandwidth increases significantly as the number of split ring resonators turn increases from one to two turns, but only slightly changes when the number of split ring resonators turn increases from two to three turns.

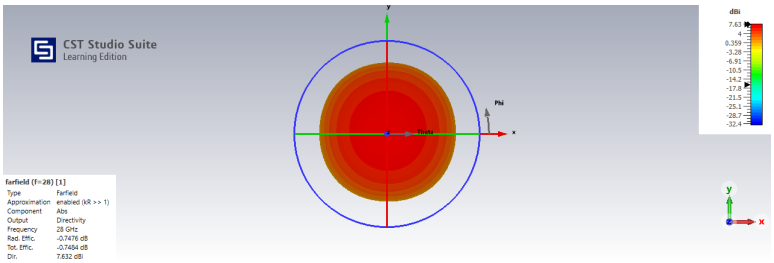

Figure 4.10: directivity of circular split ring resonator based microstrip antenna for N=3

The directivity of the circular split ring resonator-based microstrip antenna is 7.44dBi, as seen in the three-dimensional far-field radiation pattern images.

Radiation efficiency of circular split ring resonator based microstrip antenna 87.9% and total efficiency of the circular based split ring resonator microstrip antenna 87.89%. Radiation efficiency of CSRR based microstrip antenna is better than the conventional microstrip antenna. The permeability value of circular split ring resonator based microstrip antenna enhance negative value that indicate characteristic of metamaterial

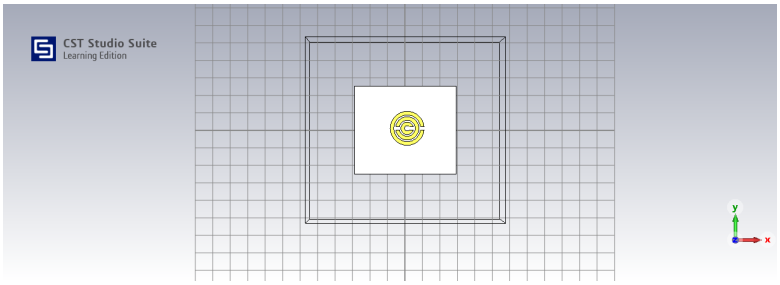

Figure 4.11: image of circular split ring resonator based microstrip antenna for N=3

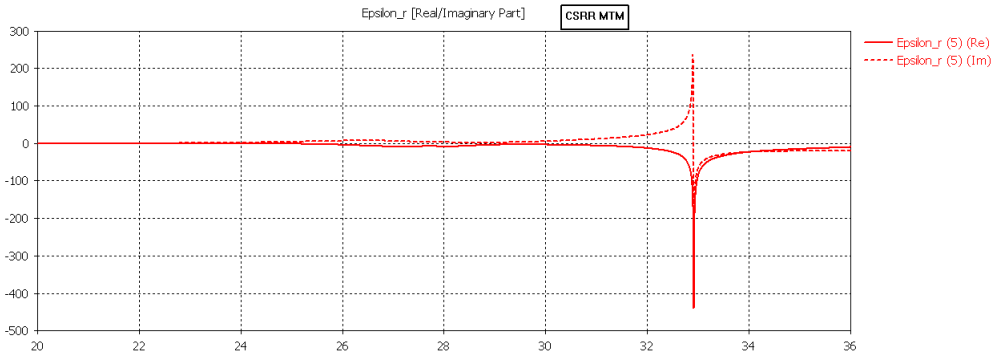

Figure 4.12: permitivity of circular split ring resonator based microstrip antenna for N=3

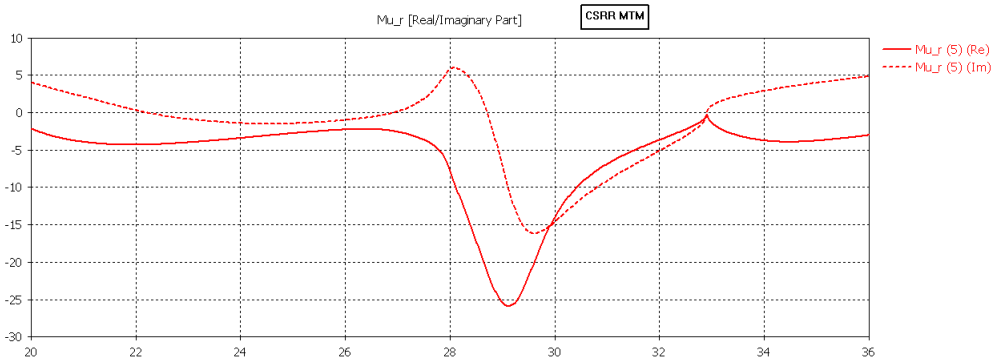

Figure 4.13: permability of circular split ring resonator based microstrip antenna for N=3

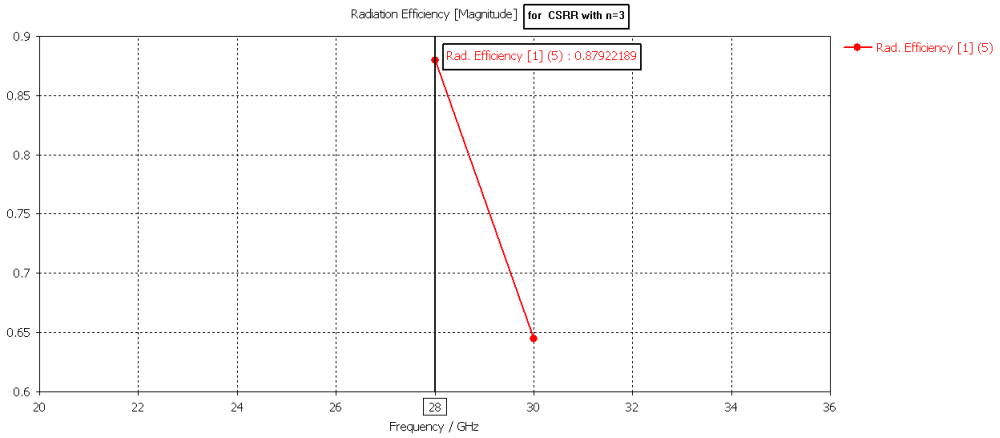

Figure 4.14: radaition efficiency of circular split ring resonator based microstrip antenna for N=3

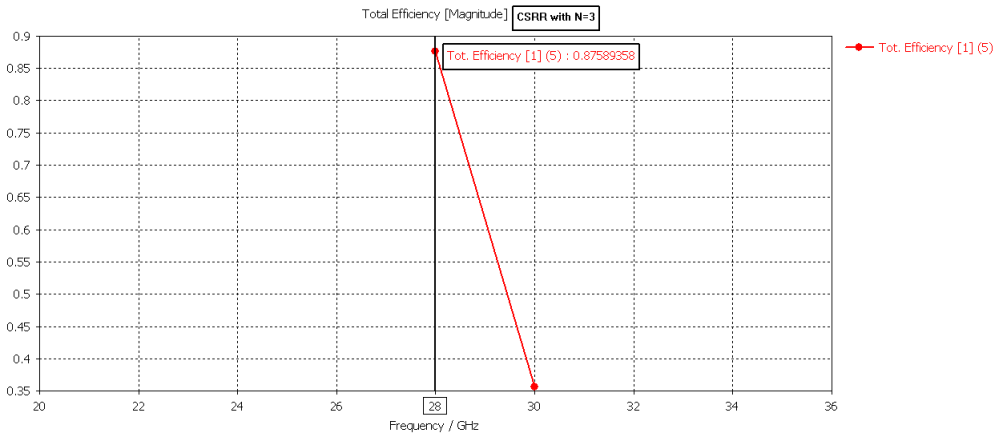

Figure 4.15: total efficiency of circular split ring resonator based microstrip antenna for N=3

4.2.2 Rectangular split ring resonator based microstrip patch antenna

for N=1

Rectangular split ring resonator-based microstrip antennas with single turns have a bandwidth 1.294 GHz (4.62%), with a frequency range of 27.269 GHz to 28.562 GHz. In comparison to a traditional microstrip antenna, the bandwidth was increased by 14.79 % that optimized with additional 0.167 GHz bandwidth.

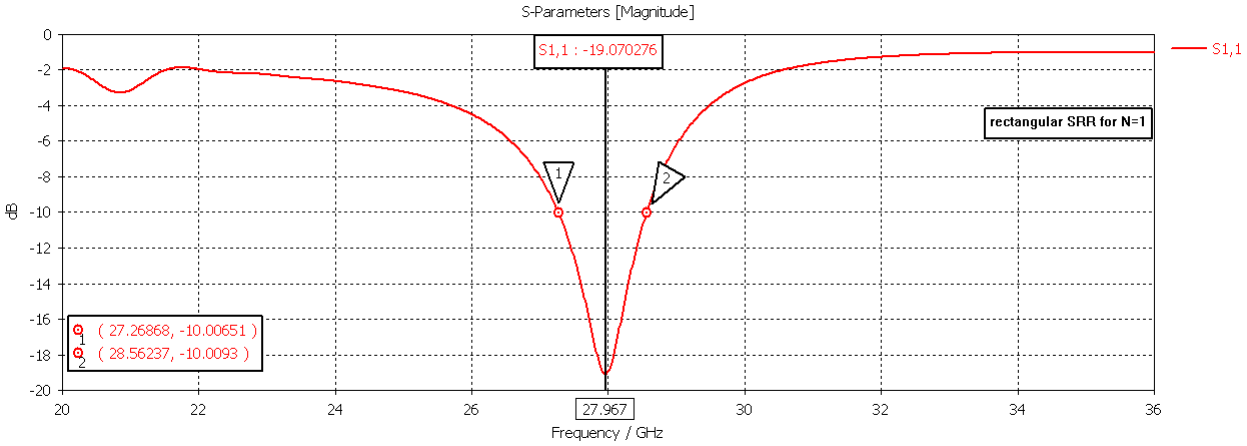

Figure 4.16: S-parameter of rectangular split ring resonator based microstrip antenna for N=1

for N=2

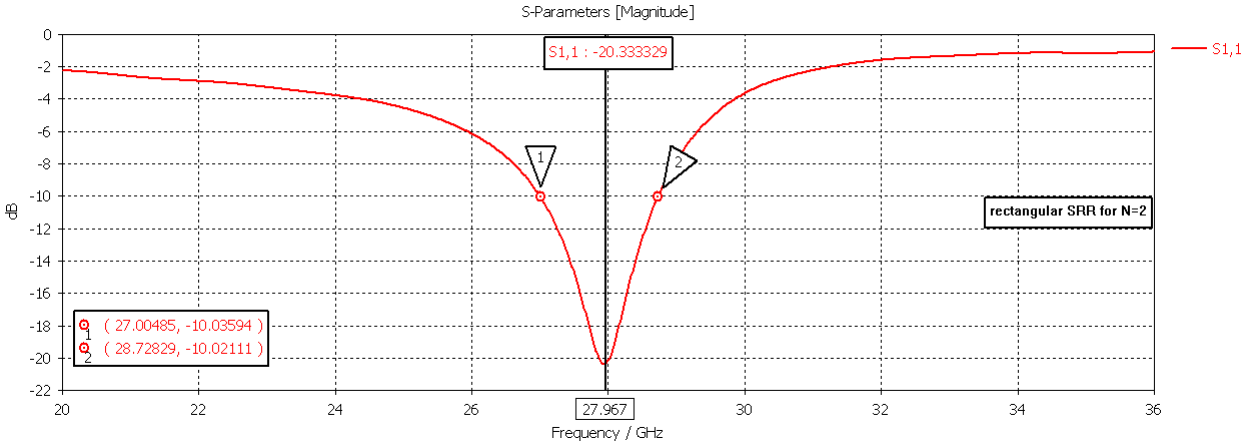

Figure 4.17: S-parameter of rectangular split ring resonator based microstrip antenna for N=2

Two-turn rectangular split ring resonator-based microstrip antennas span a frequency range of 27.00 GHz to 28673 GHz, have operating bandwidth of 1.7234 GHz (6.155%), the bandwidth was enhanced by (0.6GHZ) 52.92 % as compared to a conventional microstrip antenna. When compared to a rectangular split ring resonator with a single turn, the bandwidth increased by 13.64 % for microstrip antennas with two turns of RSRR.

for N=3

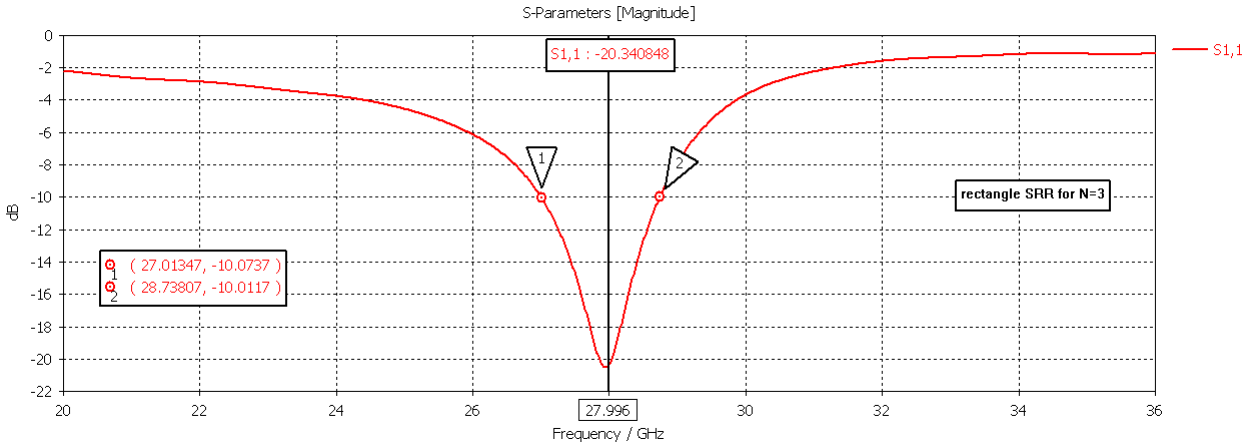

Figure 4.18: S-parameter of rectangular split ring resonator based microstrip antenna for N=3

The frequency range of operation for three-turn rectangular split ring resonator microstrip antennas is 27.0139GHZ to 28.738 GHz, with an operating bandwidth of 1.725 GHz (6.16%). In comparison to a traditional microstrip antenna, there was a 53.06% increase in bandwidth (0.598GHZ). When the number of split ring resonators rises from one to two turns, the bandwidth increases dramatically; however, when the number of resonators rises from two to three turns, no changes occur.

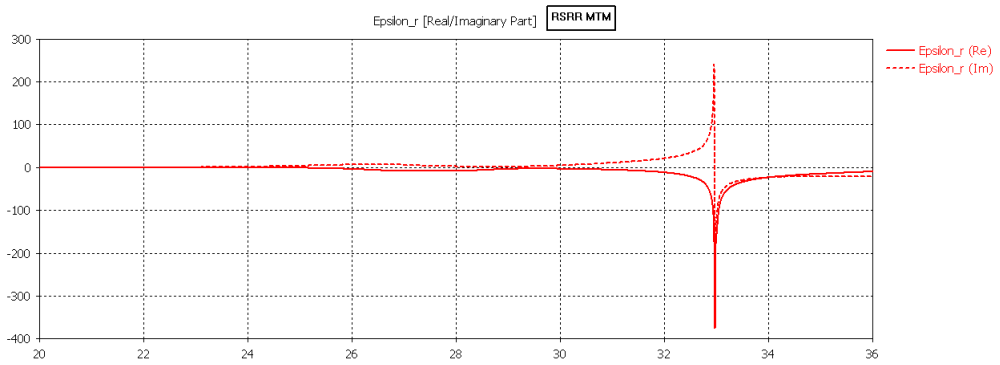

Figure 4.19: permitivity of rectangular split ring resonator based microstrip antenna for N=3

Radiation efficiency of rectangular split ring resonator based microstrip antenna 85.3% and total efficiency of the rectangular based split ring resonator microstrip antenna 84.5%.

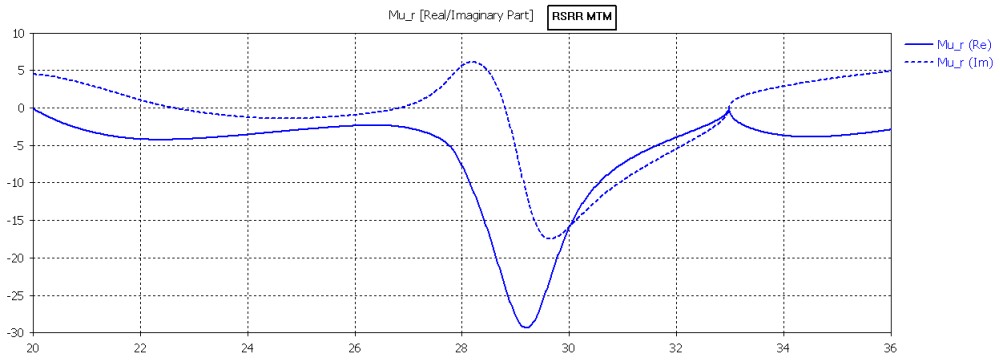

Figure 4.20: permability of rectangular split ring resonator based microstrip antenna for N=3

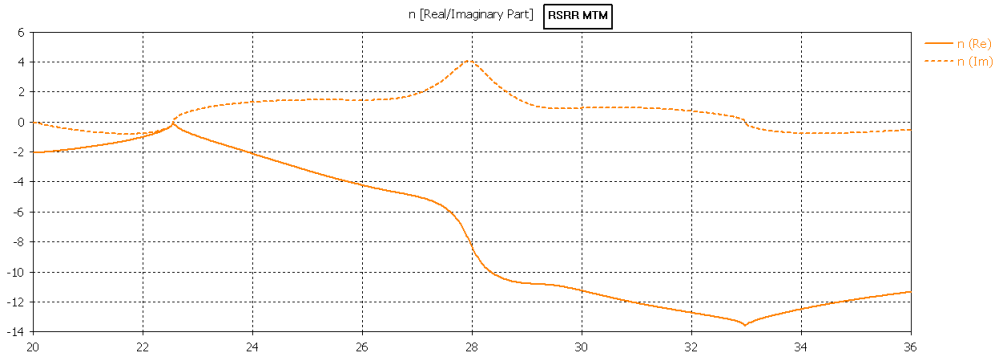

Figure 4.21: refractive index of rectangular split ring resonator based microstrip antenna for N=3

Radiation efficiency of RSRR based microstrip antenna is less than the conventional microstrip antenna. The permeability value of rectangular split ring resonator based microstrip antenna enhance negative value that indicate characteristic of metamaterial

The directivity of the rectangular split ring resonator-based microstrip antenna is 7.58 dBi, as seen in the three-dimensional far-field radiation pattern images.

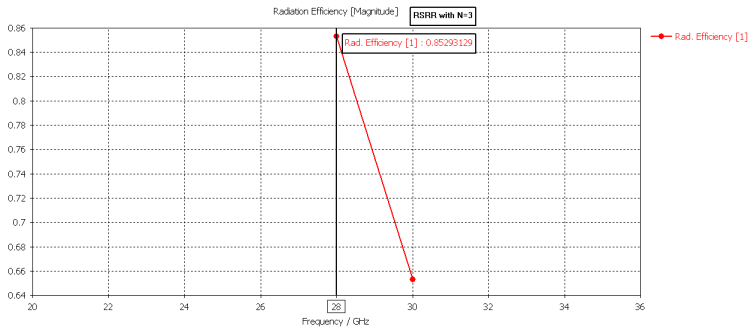

Figure 4.22: radaition efficiency of rectangular split ring resonator based microstrip antenna for N=3

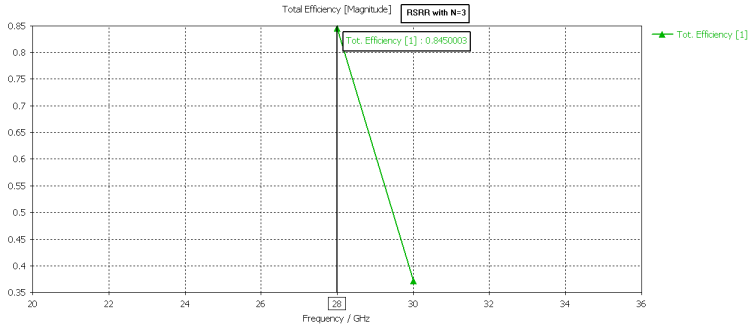

Figure 4.23: total efficiency of rectangular split ring resonator based microstrip antenna for N=3

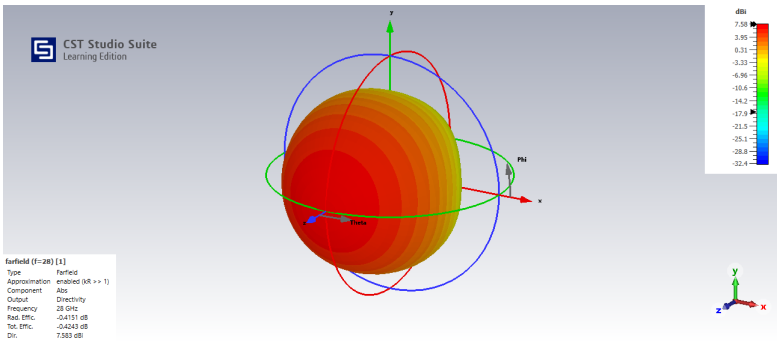

Figure 4.24: directivity of rectangular split ring resonator based microstrip antenna for N=3

4.2.3 Triangular split ring resonator based microstrip patch antenna

for N=3

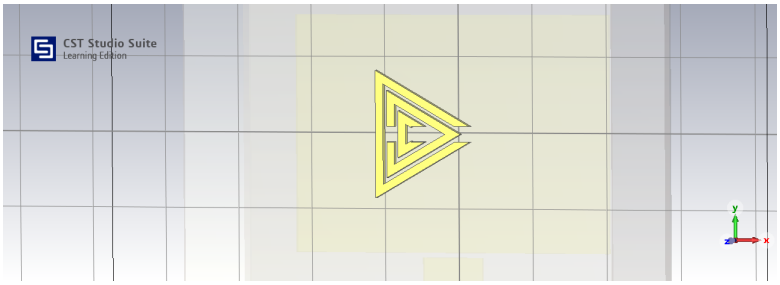

Figure 4.25: image of triangular split ring resonator based microstrip antenna for N=3

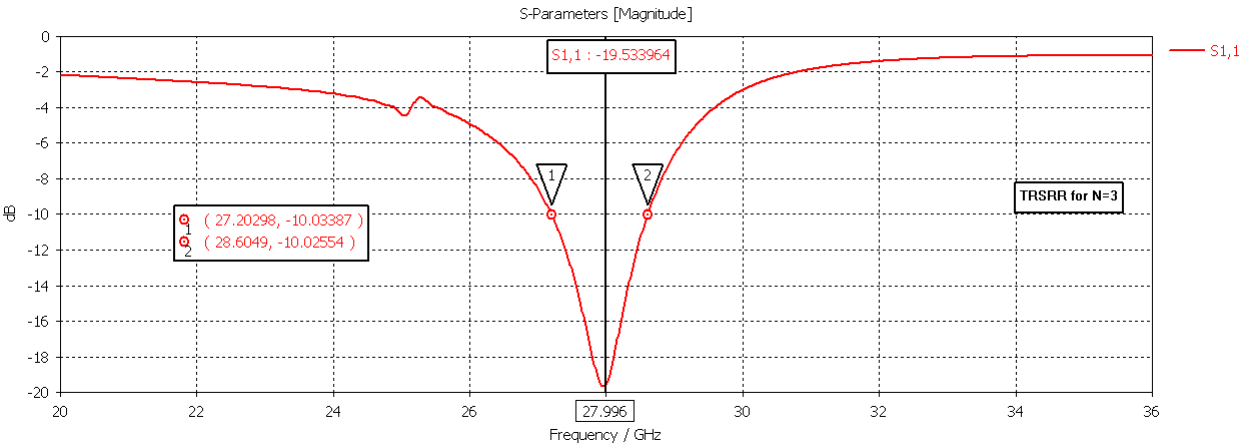

Figure 4.26: S-parameter of triangular split ring resonator based microstrip antenna for N=3

triangular split ring resonator-based microstrip antennas with three turns have a bandwidth 1.4 GHz (5%), with a frequency range of 27.203 GHz to 28.605 GHz. In comparison to a traditional microstrip antenna, the bandwidth was increased by 26.89% (0.273 GHz).

Radiation efficiency of triangular split ring resonator based microstrip antenna 80.3% and total efficiency of the triangular based split ring resonator microstrip antenna 90.69%. Radiation efficiency of TSRR based microstrip antenna is better than the conventional microstrip antenna. The permeability value of triangular split ring resonator based microstrip antenna enhance negative value that indicate characteristic of metamaterial

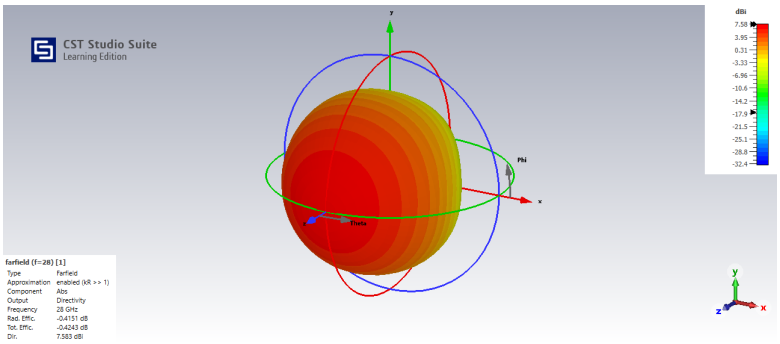

Figure 4.27: directivity of triangular split ring resonator based microstrip antenna for N=3

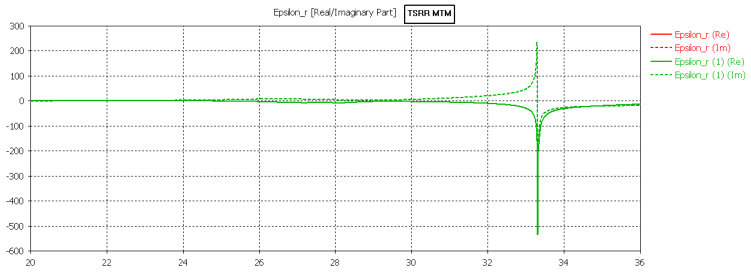

Figure 4.28: permitivity of triangular split ring resonator based microstrip antenna for N=3

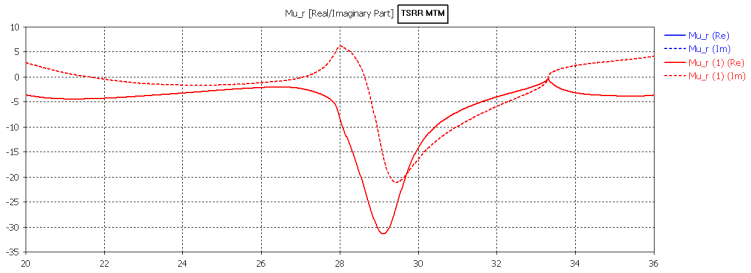

Figure 4.29: permability of triangular split ring resonator based microstrip antenna for N=3

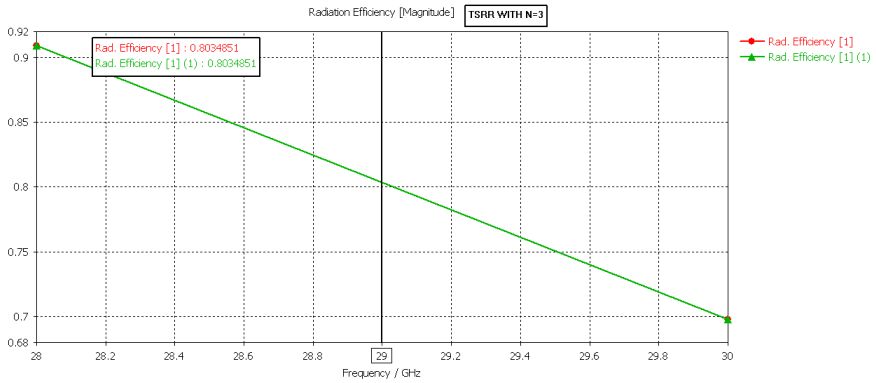

Figure 4.30: radaition efficiency of triangular split ring resonator based microstrip antenna for N=3

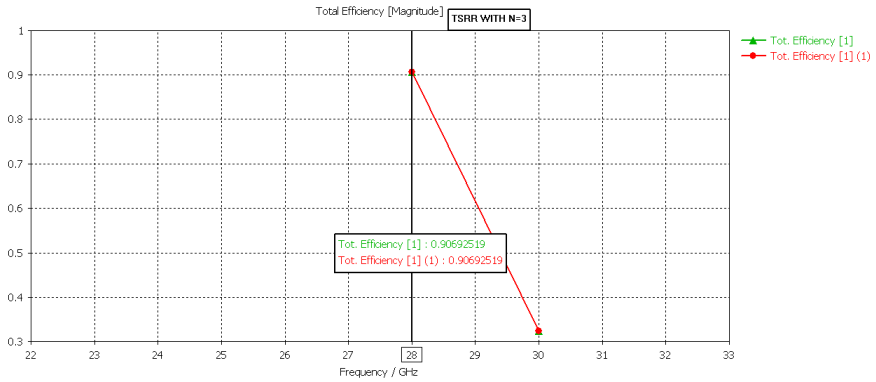

Figure 4.31: total efficiency of triangular split ring resonator based microstrip antenna for N=3.

4.2.4 Pentagonal split ring resonator based microstrip patch antenna

for N=1

Pentagonal split ring resonator-based microstrip antennas with single turns have a bandwidth 1.359 GHz (4.85%), with a frequency range of 27.209 GHz to 28.552 GHz. In comparison to a traditional microstrip antenna, the bandwidth was increased by 20.5 % that have additional 0.232 GHz bandwidth.

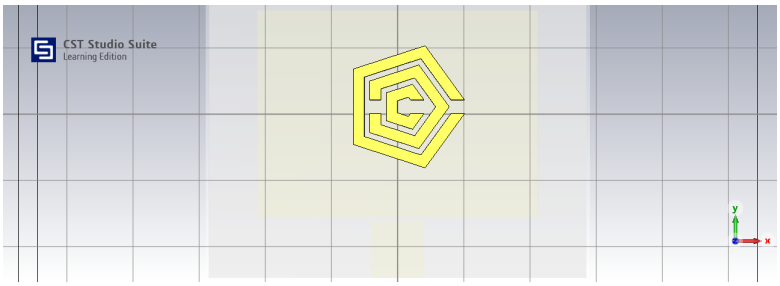

Figure 4.32: image of pentagonal split ring resonator based microstrip antenna for N=3

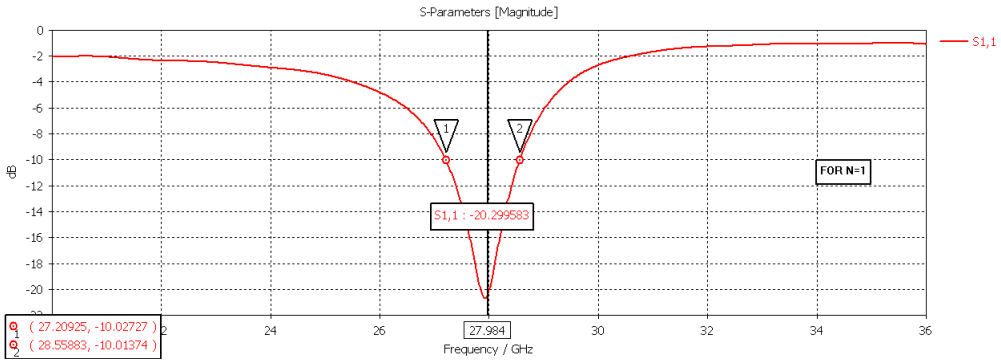

Figure 4.33: S-parameter of pentagonal split ring resonator based microstrip antenna for N=1

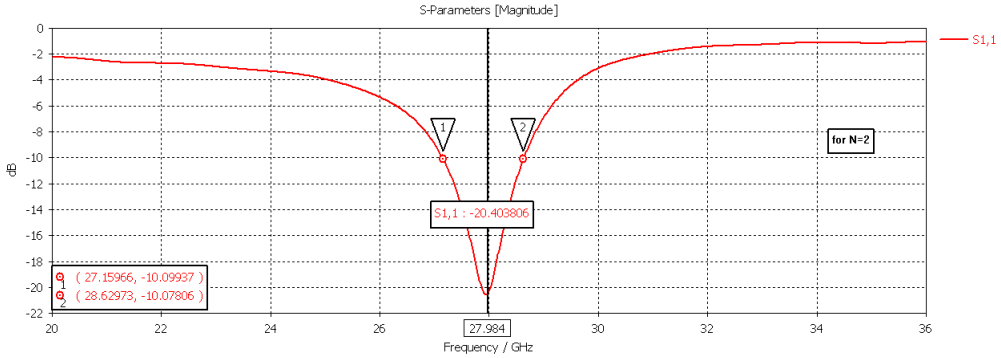

Figure 4.34: S-parameter of pentagonal split ring resonator based microstrip antenna for N=2

for N=2

Two-turn pentagonal split ring resonator-based microstrip antennas span a frequency range of 27.1596 GHz to 28.63 GHz, have operating bandwidth of 1.47 GHz (5.25 %), the bandwidth was enhanced by (0.343GHZ) 30.43 % as compared to a conventional microstrip antenna. When compared to a split ring resonator with a single turn, the bandwidth increased by 8.167 % for microstrip antennas with two turns of PSRR.

for N=3

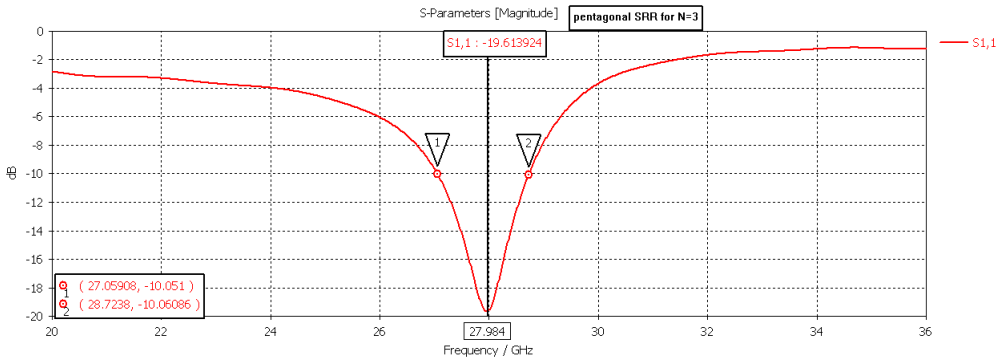

Figure 4.35: S-parameter of pentagonal split ring resonator based microstrip antenna for N=3

Three-turn pentagonal split ring resonator microstrip antennas operate in the frequency range of 27.059 GHz to 28.724 GHz and have an operating bandwidth of 1.664 GHz (5.94%). Compared to a conventional microstrip antenna, the bandwidth was increased by (0.537GHZ) 47.65%. Microstrip antennas with two turns of PSRR had a 13.2% increase in bandwidth when compared to a split ring resonator with two turns. The bandwidth increases significantly as the number of split ring resonators increases from one to two turns, but only slightly changes when the number of resonators increases from two to three turns.

Radiation efficiency of pentagonal split ring resonator based microstrip antenna 92.42% and total efficiency of the pentagonal based split ring resonator microstrip antenna 91.5%. Radiation efficiency of PSRR based microstrip antenna is better than the conventional microstrip antenna. The permeability value of pentagonal split ring resonator based microstrip antenna enhance negative value that indicate characteristic of metamaterial.

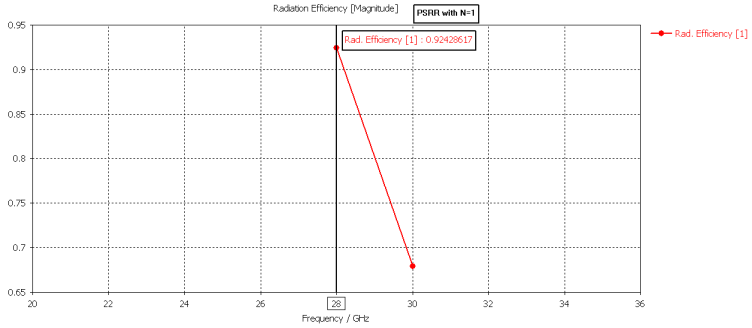

Figure 4.36: radaition efficiency pentagonal split ring resonator based microstrip antenna for N=3

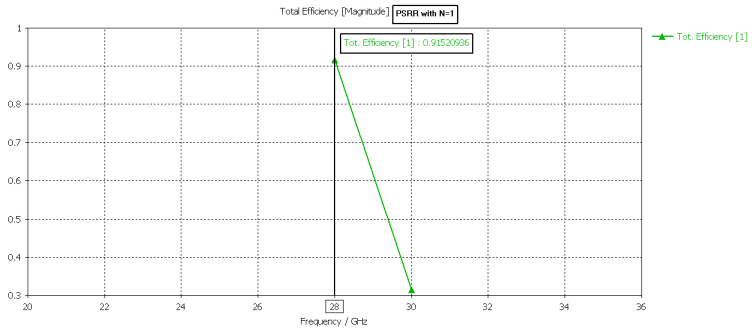

Figure 4.37: total efficiency of pentagonal split ring resonator based microstrip antenna for N=3

4.3 Performance comparison of metamaterial-based microstrip antennas using different numbers of split ring resonator elements

4.3.1 For single rectangular split ring resonator based microstrip antenna

The frequency range of operation for three-turn of single rectangular split ring resonator microstrip antennas is 27.0139 to 28.738 GHz, with an operating bandwidth of 1.725 GHz (6.16%).

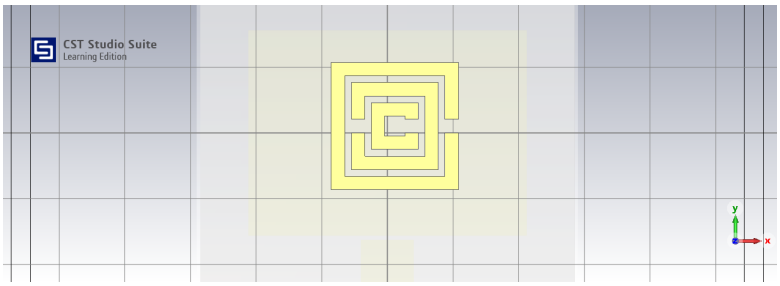

Figure 4.38: image of rectangular split ring resonator based microstrip antenna for N=3

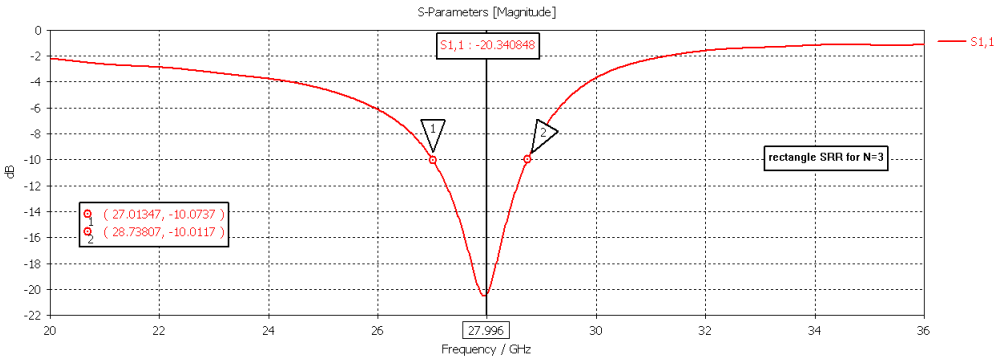

Figure 4.39: S-parameter of rectangular split ring resonator based microstrip antenna for N=3

4.3.2 For double rectangular split ring resonator based microstrip antenna

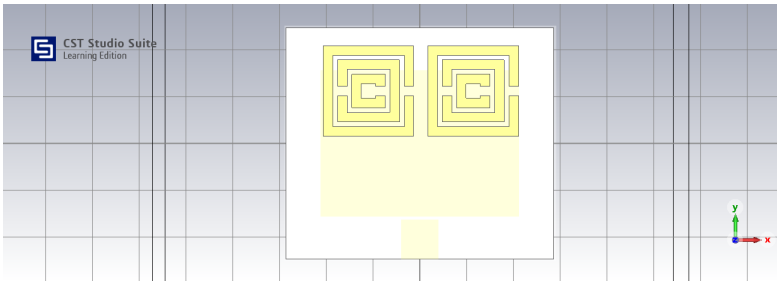

Figure 4.40: image of two rectangular split ring resonator based microstrip antenna for N=3

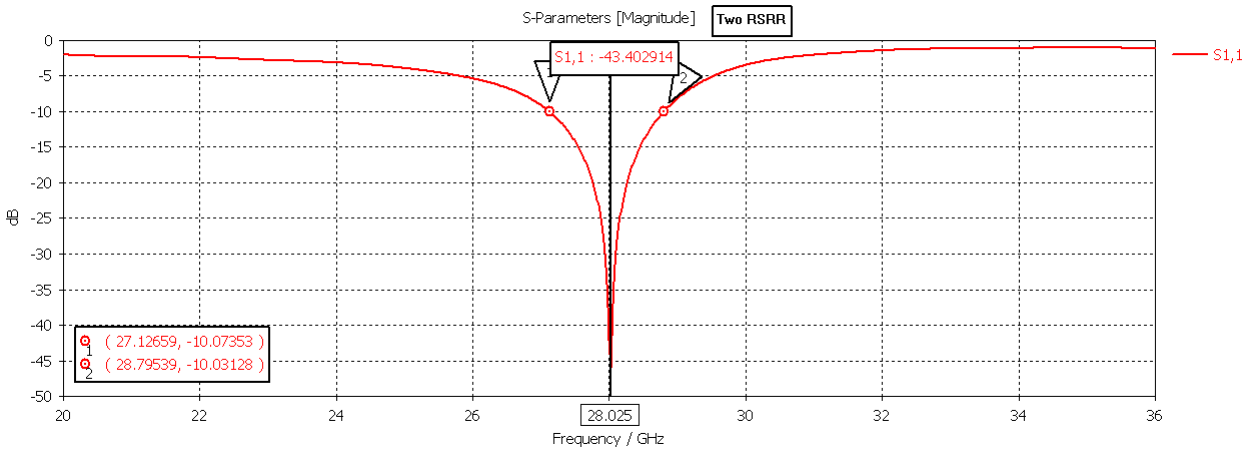

Figure 4.41: S-parameter of two rectangular split ring resonator based microstrip antenna for N=3

The frequency range of operation for three-turn of double elements rectangular split ring resonator microstrip antennas is 27.1266 GHZ to 28.7954 GHz, with an operating bandwidth of 1.669 GHz (5.96 %).

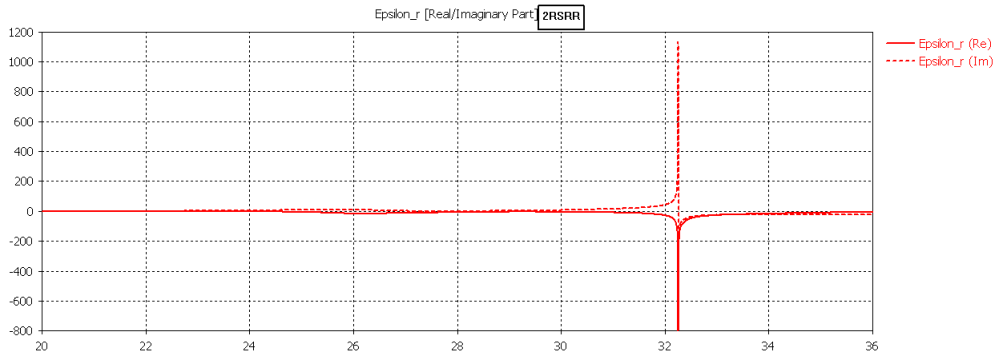

Figure 4.42: permitivity of two rectangular split ring resonator based microstrip antenna for N=3

Radiation efficiency of two rectangular split ring resonator based microstrip antenna 91.2 % and total efficiency of the two rectangular based split ring resonator microstrip antenna 88.39 %. Radiation efficiency of 2 RSRR based microstrip antenna is better than the conventional microstrip antenna. The permeability value of two rectangular split ring resonator based microstrip antenna enhance negative value that indicate characteristic of metamaterial.

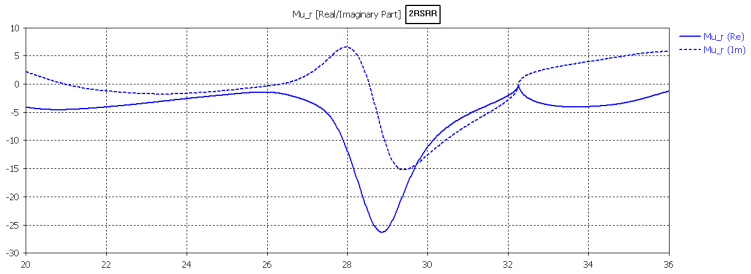

Figure 4.43: permability of two rectangular split ring resonator based microstrip antenna for N=3

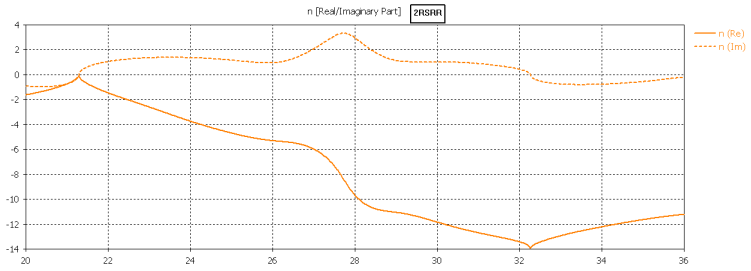

Figure 4.44: refractive index of two rectangular split ring resonator based microstrip antenna for N=3

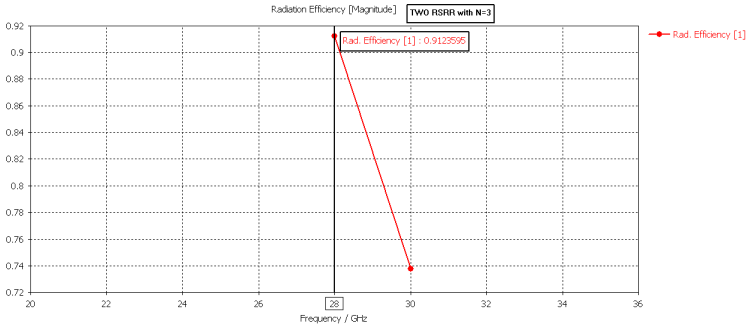

Figure 4.45: radaition efficiency of two rectangular split ring resonator based microstrip antenna for N=3

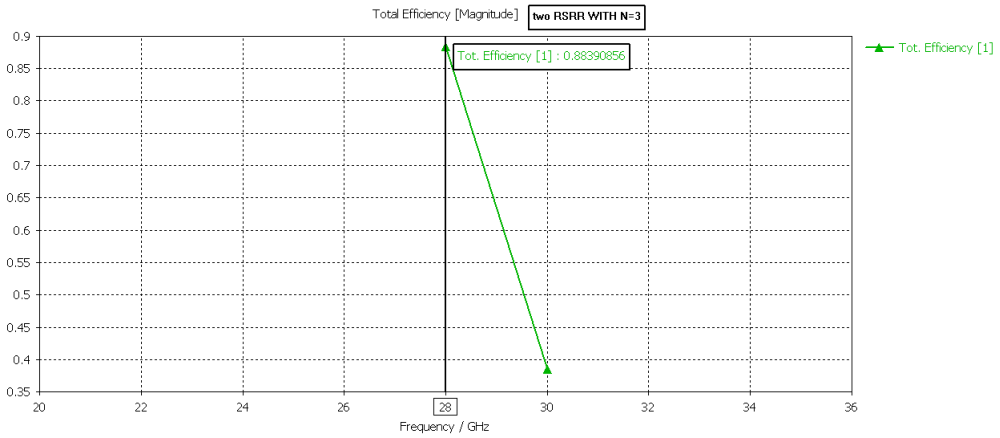

Figure 4.46: total efficiency of two rectangular split ring resonator based microstrip antenna for N=3

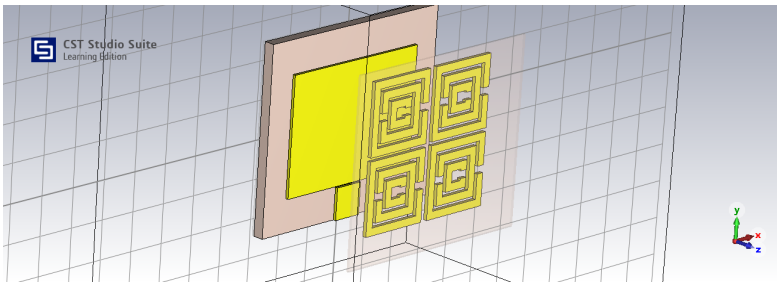

Figure 4.47: image of four rectangular split ring resonator based microstrip antenna for N=3

4.3.3 For 2x2 four rectangular split ring resonator based microstrip antenna

The 2x2 four-element rectangular SRR bandwidth of the MTM-based microstrip antenna is 2.23 GHz. The bandwidth was enhanced by 101.81% as compared to a conventional microstrip antenna without SRR.

Radiation efficiency of four rectangular split ring resonator based microstrip antenna 93.07 % and total efficiency of the four rectangular based split ring resonator microstrip antenna 92.54 %. Radiation efficiency of 4 RSRR based microstrip antenna is better than the conventional microstrip antenna. The permeability value of four rectangular split ring resonator based microstrip antenna enhance negative value that indicate characteristic of metamaterial.

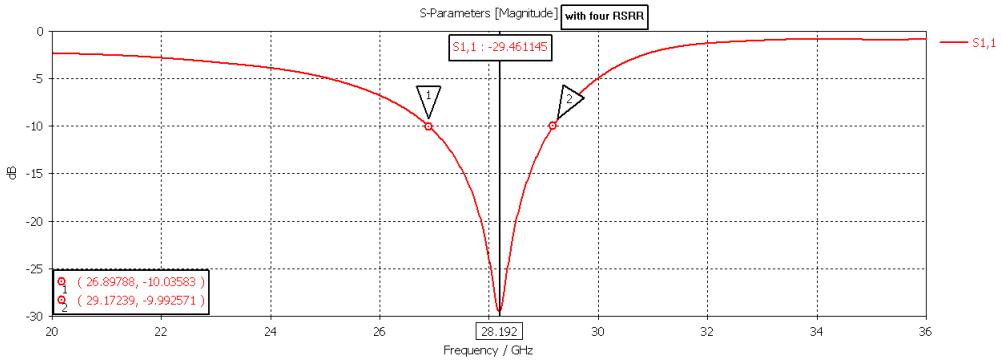

Figure 4.48: S-parameter of four rectangular split ring resonator based microstrip antenna for N=3

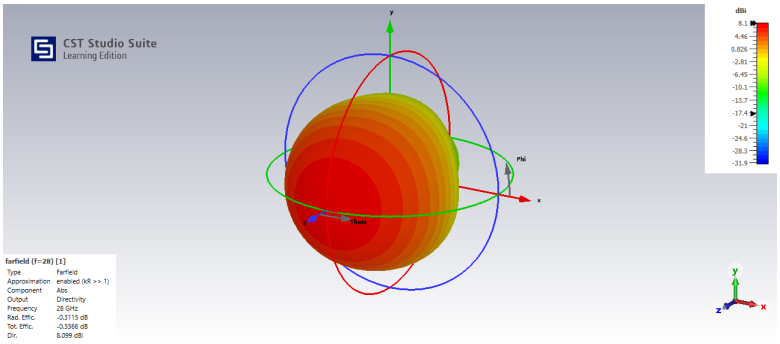

Figure 4.49: directivity of four rectangular split ring resonator based microstrip antenna for N=3

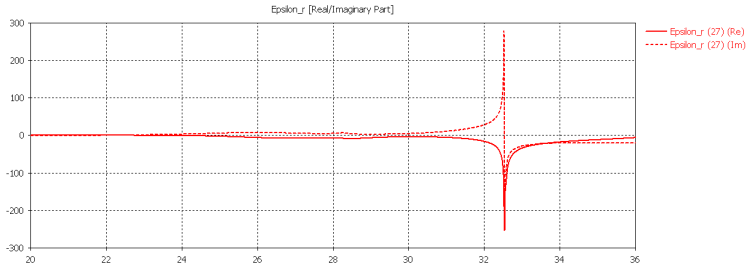

Figure 4.50: permitivity of four rectangular split ring resonator based microstrip antenna for N=3

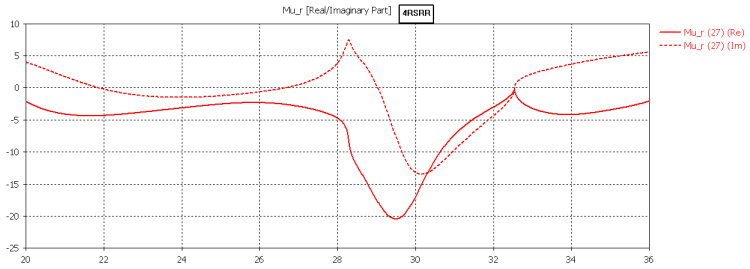

Figure 4.51: permability of four rectangular split ring resonator based microstrip antenna for N=3

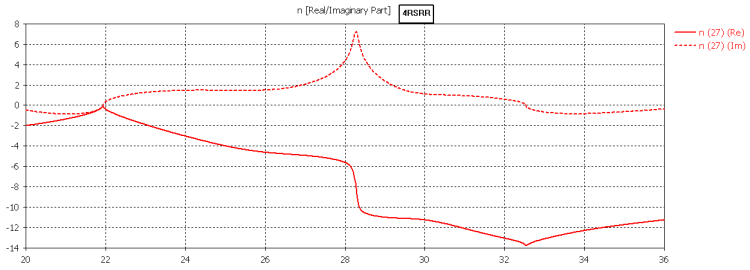

Figure 4.52: refractive index of two rectangular split ring resonator based microstrip antenna for N=3

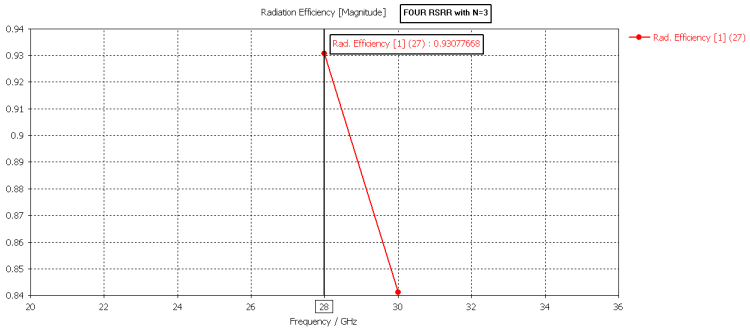

Figure 4.53: radaition efficiency of two rectangular split ring resonator based microstrip antenna for N=3

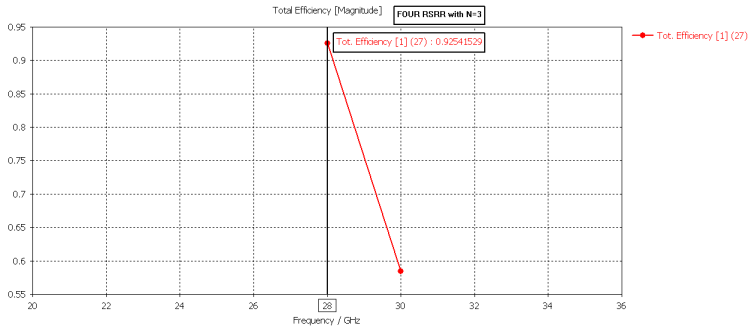

Figure 4.54: total efficiency of four rectangular split ring resonator based microstrip antenna for N=3

Table 4.1: Summary of simulation results

Type of antennas	No of turn(N)	Bandwidth(GHZ)	Radiation eff(%)
Conventional		1.127	86
CSRR based microstrip antenna	N1	1.36	86
CSRR based microstrip antenna	N2	1.535	
CSRR based microstrip antenna	N3	1.652	87.9
RSRR based microstrip antenna	N1	1.294	
RSRR based microstrip antenna	N2	1.7234	
RSRR based microstrip antenna	N3	1.725	85.3
TSRR based microstrip antenna	N3	1.4	80.3
PSRR based microstrip antenna	N1	1.359	
PSRR based microstrip antenna	N2	1.472	
PSRR based microstrip antenna	N3	1.664	92.42
two RSRR based microstrip antenna	N3	1.669	91.2
four RSRR based microstrip antenna	N3	2.23	93.07

Chapter 5: Conclusion and Recommendation on Future Work

5.1 Conclusion

Metamaterial based microstrip antenna have better bandwidth than the conventional microstrip antenna. With an increase in turns, the MTM-based microstrip antenna's bandwidth expanded for every SRR segmentation. Notably, it changed quickly from N=1 to N=2, but only marginally after that.
Compared to circular, triangular, and pentagonal split ring resonator; rectangular SRRs exhibit superior bandwidth augmentation.
By etching the rectangular, circular triangular, and pentagonal SRRs, respectively, with N=3, the bandwidth is increased by 53.06%, 46.7%, 26.89%, and 47.65 % compared to the conventional microstrip antenna.
The bandwidth is enhanced by using more split ring resonators than by using just one. The bandwidth is increased by 101.81% when utilizing 2x2 SRR elements compared to a conventional microstrip antenna without a split ring resonator.
Conventional microstrip antenna, CSRR based microstrip antenna, rectangular split ring resonator based microstrip antenna, TSRR based microstrip antenna and PSRR based micro strip antenna have radiation efficiency of 86 %, 87.9 %, 85.3 %, 80.3 % and 92.4 % respectively. RSRR based microstrip based antenna have less radiation efficiency compared to the conventional microstrip antenna and other MTM based microstrip antenna and PSRR based microstrip antenna enhance higher radiation efficiency.
The bandwidth is enhanced by using more split ring resonators than by using just one. The bandwidth is increased by 101.81% when utilizing 2x2 SRR elements compared to a conventional microstrip antenna without a split ring resonator.
The radiation efficiency is enhanced by using more split ring resonators than by using just one. The radiation efficiency of two RSRR is 91.2 % and for four RSRR IS 93.07 %. The radiation efficiency is increased with increased number of split ring resonator.

5.2 Recommendation for Future Work

The following areas of study are worthy of consideration to carry out further study.

First, an experimental demonstration of the effect of a person, hand- and body-effect, on the signal propagation between the transmitter and the receiver should be presented in the future work.

Moreover, the researcher can increase the array size to further improve the antenna performance.

Finally, it is recommended to develop practical infrastructure of the above designed antenna systems to optimize for local market technology transformation.

Bibliography

[1] M. Nabil, *Design, Simulation and Analysis of a High Gain Small Size Array Antenna for 5G Wireless Communication* (Wireless Personal Communications, 2020).

[2] A. Pandey, *Practical Microstrip and Printed Antenna Design* (boston,london: artech house, 2019).

[3] R. Bancroft, *Rectangular Microstrip Antennas* (in Microstrip and Printed Antenna Design, USA, SciTech Publishing Inc, 2009, p. 11).

[4] V. H. R, *V. H. R, Comparative Study of Square and Circular Split Ring Resonator Metamaterial for Patch Antenna Miniaturization for C-band Wireless Applications, University of Canberra. UTC from IEEE Xplore, 2019.*

[5] C. . A. M. Ali, Dual-band millimeter-wave microstrip patch array antenna for 5G smartphones, *(In Paper presented at the international conference on advanced science and engineering, Zakho, Duhok, Iraq).*

[6] 1. M. J. A. Muhammad M. Hossain Orthogonal Printed Microstrip Antenna Arrays for 5G Millimeter-Wave Applications *(AEU International Journal of Electronics and Communications. https://doi.org/10.1016/j., . 2022 Jan; 13(1): 53).*

*[7] R. P. A. K. G. K. Twinkal Rao,*Design a Wideband Aperture Coupled Stacked *(INTERNATIONAL JOURNAL OF SCIENTIFIC PROGRESS AND RESEARCH (IJSPR), vol. Volume 74, no. Issue 174 Number 01, 2020.).*

[8] S. U. 1. A. bJalal Khan, Design of a Millimeter-Wave MIMO Antenna Array for 5G Communication Terminals *(4 April 2022).*

[9] P. K. a. T. A. Bukola Ajewole, A Microstrip Antenna Using I-Shaped Metamaterial Superstrate with Enhanced Gain for Multiband Wireless Systems *(micromachine, 2023).*

[10] T. B. M. B. T. . R. R. Prabu, Design of 5G mm-wave antenna using line feed and corporate feed techniques *(In Proceedings of the second international conference on SCI 2018, vol. vol 1, p. (pp. 367–380)., 2019).*

[11] Mao, C., Khalily, M., Xiao, P., Brown, T., Gao, S, Planar sub-millimeter-wave array antenna with enhanced gain and reduced sidelobes for 5G broadcast applications *(IEEE Transactions on Antennas and Propagation, 67,, p. 160–168, 2019).*

[12] N. A.-Y. Y. Ojaroudi Parchin, Frequency reconfigurable antenna array for MM-wave 5G mobile handsets *(In Paper presented at the broadband communications, networks, and systems, Cham, 2019).*

[13] Muhammad Nauman, Muddasir Abbas ***Simple High Gain Array Antenna for 5G Applications****, (International Journal of Engineering Research Technology (IJERT), vol. Vol. 9, no. Issue 09, September-2020)*

[14] Warren L. Stutzman, Gary A. Thiele antenna theory and design *(united state of america: , John Wiley Sons, Inc, 2012).*

[15] D. V. a. P. K. N. Chavda Designing of microstrip patch antenna for 3g-wcdma applications *(International Advanced Research Journal in Science, Engineering and Technology, Vols. ,vol. 1, p. pp. 49–53, ,2012).*

[16] A. Fatthi Alsager design and analysisi of microstrip patch antenna arrays *(2011).*

[17] http://en.wikipedia.org/wiki/ ***Metamaterial in 53. SPIE Press, Bellingham, WA, USA , 2003****, in 53. SPIE Press, Bellingham, WA, USA (2003).*

[18] Tie Jun Cui · David R. Smith · Ruopeng Liu Metamaterials Theory, Design and Applications *(newyork: springer, 2010).*

[19] PRAVEEN KUMAR ,ANWEER ALI Electromagnetic Metamaterials: A New-Paradigm of Antenna Design *(IEEE ACCESS, vol. 9, p. 18722, 2021).*

[20] Chen, K.; Yang, Z.; Feng, Y.; Zhu, B.; Zhao, J.; Jiang, T. Improving microwave antenna gain and bandwidth with phase compensation metasurface *(AIP adv, 2015).*

[21] Vallappil, A.K.; Rahim, M.K.A.; Khawaja, B.A.; Iqbal, M.N. Compact Metamaterial Based Butler Matrix With Improved Bandwidth for 5G Applications *(IEEE Access, vol. 1, p. 13573–13583., 2020).*

[22] C. A. Balanis, John Wiley Sons. Antenna Theory: Analysis and Design: *(2012).*

[23] C. C. a. T. I. A. Sanada, NOVEL ZEROTH-ORDER RESONANCE IN COMPOSITE RIGHT/LEFT-HANDED TRANSMISSION LINE RESONATORS, NOVEL ZEROTH-ORDER RESONANCE IN COMPOSITE RIGHT/LEFT-HANDED TRANSMISSION LINE RESONATORS *(In Proc. Asia-Pacific Microwave Conference, 2003).*

[24] S. Liao, Q. Xue, and J. Xu,Parallel-Plate Transmission Line and L-Plate Feeding Differentially Driven H-Slot Patch Antenna, Parallel-Plate Transmission Line and L-Plate Feeding Differentially Driven H-Slot Patch Antenna *(IEEE Antennas and Wireless Propagation Letters, vol. vol. 11, pp. pp. 640-644,, 2012).*

[25] F. J. Herraiz-Martinez, V. Gonzalez-Posadas, L. E. Garcia-Munoz etal Multifrequency and Dual-Mode Patch Antennas Partially Filled With Left-Handed

[26] S. Yan METAMATERIAL DESIGN AND ITSAPPLICATION FOR ANTENNAS *(Heverlee, Belgium: KU Leuven, Science, Engineering Technology, 2015)*

[27] Q. Wu, P. Pan, F. Y. Meng et al. A novel flat lens horn antenna designed based on zero refraction principle of metamaterials *(Applied Physics A,, vol. vol. 87, no. no. 2, , pp. pp. 151-156, 2007)*

[28] P. J. F. Gonz´alez, Multifunctional Metamaterial Designs for Antenna Applications *(barcelona, 2015)*

[29] 1. M. J. A. Muhammad M. Hossain, Orthogonal Printed Microstrip Antenna Arrays for 5G Millimeter-Wave Applications *(Micromachines (Basel), . 2022 Jan; 13(1): 53.)*

[30] Weiglhofer, W.S., Lakhtakia, A, to complex mediums for optics and electromagnetics.

[31] Liu, Tie Jun Cui · David R. Smith · Ruopeng, Metamaterials Theory, Design, and Applications *(Micromachines (Springer New York Dordrecht Heidelberg London: 2010.)*